

# BPS and non-BPS kinks in a massive non-linear $\mathbb{S}^2$ -sigma model

A. Alonso-Izquierdo<sup>a</sup>, M. A. Gonzalez Leon<sup>a</sup> and J. Mateos Guilarte<sup>b</sup>

<sup>a</sup> *Departamento de Matematica Aplicada and IUFFyM, Universidad de Salamanca, SPAIN*

<sup>b</sup> *Departamento de Fisica and IUFFyM, Universidad de Salamanca, SPAIN*

The stability of the kinks of the non-linear  $\mathbb{S}^2$ -sigma model discovered in [1] is discussed from several points of view. After a direct estimation of the spectra of the second-order fluctuation operators around topological kinks, first-order field equations are proposed to distinguish between BPS and non-BPS kinks. The one-loop mass shifts caused by quantum fluctuations around the topological kinks are computed using the Cahill-Comtet-Glauber formula [2]. The (lack of) stability of the non-topological kinks is unveiled by application of the Morse index theorem. These kinks are identified as non-BPS states and the interplay between instability and supersymmetry is explored.

PACS numbers: 11.10. Lm , 11.27. +d, 75.10. Pq

## I. INTRODUCTION

The main theme in this paper is the analysis of the structure of the manifold of kink solitary waves discovered in [1]. In particular, we shall offer a full description of the stability of the different type of kinks. As a bonus, we shall gain information about the semi-classical behavior of such kinks from the stability analysis, providing us with enough data to compute the one-loop mass shifts for the topological kinks. We shall also propose first-order field equations that are solved by a single type of BPS topological kinks as well as the time-dependent Q-kinks, which arise when the masses of the fundamental quanta are equal. The first-order equations are linked to topological bounds leading to another route to study stability.

Prior to our work [1], kinks in massive non-linear sigma models have been known for some time and profusely studied in different supersymmetric models under the circumstance that all the masses of the pseudo Nambu-Goldstone particles are equal. The study started with two papers by Abraham and Townsend [3], [4] in which the authors discovered a family of Q-kinks in a (1+1)-dimensional  $\mathcal{N} = (4, 4)$  supersymmetric non-linear sigma model with a hyper-Kahler Gibbons-Hawking instanton as the target space and mass terms obtained from dimensional reduction. In [5], however, these kinks were re-considered by constructing the dimensionally reduced supersymmetric model by means of the mathematically elegant technique of hyper-Kahler quotients. By doing this, the authors deal with massive  $\mathbb{C}P^N$  or  $\mathbb{H}P^N$  models, a playground closer to our simpler massive  $\mathbb{S}^2$ -sigma model. Similar  $\mathcal{N} = 2$  BPS walls in the  $\mathbb{C}P^1$ -model with twisted mass were described in [6]. In a parallel development in the (2+1)-dimensional version of these models, two-dimensional Q-lumps were discovered in [7] and [8]. Throughout this field, the most interesting result is the demonstration in [9] and [10] that composite solitons in  $d = 3 + 1$  of Q-strings and domain walls are exact BPS solutions that preserve  $\frac{1}{4}$  of the supersymmetries: ( See also the review [11], where a summary of these supersymmetric topological solitons is offered.)

Our investigation differs from previous work in the area

of topological defects in non-linear sigma models in two important aspects: 1) We remain in a purely bosonic framework; in fact, we consider the simplest massive non-linear sigma model. 2) We study the case when the masses of the pseudo Nambu-Goldstone bosons are different. The search for kinks in the (1+1)-dimensional model (domain walls in  $d = 3 + 1$ ) is tantamount to the search for finite action trajectories in the repulsive Neumann system, a particle moving in an  $\mathbb{S}^2$ -sphere under the action of non-isotropic repulsive elastic forces. It is well known that this dynamical system is completely integrable [26], [28]. We show, however, that the problem is Hamilton-Jacobi separable by using elliptic coordinates in the sphere. Use of this allows us to find four families of homoclinic trajectories starting and ending at one of the poles which are unstable points of the mechanical system. In the field-theoretical model the poles become ground states, whereas the homoclinic trajectories correspond to four families of non-topological kinks. Each member in a family is formed by a non-linear combination of two basic topological kinks (of different type) with their centers located at any relative distance with respect each other.

It is remarkable that the static field equations of this massive non-linear sigma model are (almost) the static Landau-Lifshitz equations governing the high spin and long wavelength limit of 1D ferromagnetic materials. From this perspective, topological kinks can be interpreted respectively as Bloch and Ising walls that form interfaces between ferromagnetic domains. The structure of the variety of solitary spin waves, all of them formed by one basic Bloch wall and one basic Ising wall at different distances, is the same as the structure of the set of walls in the XY model described in [34]. Far from this non-relativistic context, degenerate Bloch/Ising branes have also been studied in two-scalar field theories coupled to gravity in [12], [13], and [14]. The brane solutions have a similar structure to the NTK kinks in this model but it is necessary to cope with a wrap factor because of the coupling to the metric tensor.

The organization of the paper is as follows: In Sections §. II, II, and IV we describe the model, unveil the topological kinks, and analyze kink stability in a direct

approach. The semi-classical masses of topological kinks are computed using the CCG formula [2]. In Section §. V the topological and  $Q$ -kinks studied in the previous Sections are tested as solution of first-order equations. Sections §. VI and VII are devoted to identifying and characterizing the rich moduli space of non-topological kinks of the model by using elliptic coordinates in the sphere. In Sections §. VIII and IX, the lack of stability of non-topological kinks is established. Section §. X shows how these kinks arise in a non-relativistic context in the disguise of solitary spin waves in ferromagnetic materials. Finally, in Section §. XI we address the question of whether or not supersymmetric extensions of this model are plausible.

## II. THE (1+1)-DIMENSIONAL MASSIVE NON-LINEAR $\mathbb{S}^2$ -SIGMA MODEL

We shall focus on the non-linear  $\mathbb{S}^2$ -sigma model studied in Reference [1]. The action governing the dynamics is:

$$S[\phi_1, \phi_2, \phi_3] = \int dt dx \left\{ \frac{1}{2} g^{\mu\nu} \sum_{a=1}^3 \frac{\partial \phi_a}{\partial x^\mu} \frac{\partial \phi_a}{\partial x^\nu} - V \right\}, \quad (1)$$

with  $V = V(\phi_1(t, x), \phi_2(t, x), \phi_3(t, x))$ . The scalar fields are constrained to satisfy:

$$\phi_1^2 + \phi_2^2 + \phi_3^2 = R^2$$

and thus  $\phi_a(t, x) \in \text{Maps}(\mathbb{R}^{1,1}, \mathbb{S}^2)$  are maps from the (1+1)-dimensional Minkowski space-time to a  $\mathbb{S}^2$ -sphere of radius  $R$ , which is the target manifold of the model.

Our conventions for  $\mathbb{R}^{1,1}$  are as follows:  $x^\mu \in \mathbb{R}^{1,1}$ ,  $\mu = 0, 1$ ,  $x^\mu \cdot x_\mu = g^{\mu\nu} x_\mu x_\nu$ ,  $g^{\mu\nu} = \text{diag}(1, -1)$ .  $x^0 = t$ ,  $x^1 = x$ ,  $x^\mu \cdot x_\mu = t^2 - x^2$ ;

$$\frac{\partial}{\partial x_\mu} \left( \frac{\partial}{\partial x^\mu} \right) = \partial_\mu \partial^\mu = g^{\mu\nu} \partial_{\mu\nu}^2 = \square = \frac{\partial^2}{\partial t^2} - \frac{\partial^2}{\partial x^2}$$

The infrared asymptotics of (1+1)-dimensional scalar field theories forbids massless particles, see [15]. We thus choose the simplest potential energy density that would be generated by quantum fluctuations giving mass to the fundamental quanta:

$$V(\phi_1, \phi_2, \phi_3) = \frac{1}{2} (\alpha_1^2 \phi_1^2 + \alpha_2^2 \phi_2^2 + \alpha_3^2 \phi_3^2), \quad (2)$$

which we set with no loss of generality such that:  $\alpha_1^2 \geq \alpha_2^2 > \alpha_3^2 \geq 0$ .

1. Solving  $\phi_3$  in favor of  $\phi_1$  and  $\phi_2$ ,  $\phi_3 = \text{sg}(\phi_3) \sqrt{R^2 - \phi_1^2 - \phi_2^2}$ , we find:

$$S = \frac{1}{2} \int dt dx \left\{ \partial_\mu \phi_1 \partial^\mu \phi_1 + \partial_\mu \phi_2 \partial^\mu \phi_2 + \frac{(\phi_1 \partial_\mu \phi_1 + \phi_2 \partial_\mu \phi_2)(\phi_1 \partial^\mu \phi_1 + \phi_2 \partial^\mu \phi_2)}{R^2 - \phi_1^2 - \phi_2^2} - V_{\mathbb{S}^2}(\phi_1, \phi_2) \right\}$$

$$V_{\mathbb{S}^2}(\phi_1, \phi_2) = \frac{1}{2} ((\alpha_1^2 - \alpha_3^2) \phi_1^2 + (\alpha_2^2 - \alpha_3^2) \phi_2^2 + \text{const.}) \simeq \frac{\lambda^2}{2} \phi_1^2(t, x) + \frac{\gamma^2}{2} \phi_2^2(t, x) \quad (3)$$

with  $\lambda^2 = (\alpha_1^2 - \alpha_3^2)$ ,  $\gamma^2 = (\alpha_2^2 - \alpha_3^2)$ ,  $\lambda^2 \geq \gamma^2$ .

2. Thus, the interactions come from the geometry:

$$\frac{(\phi_1 \partial_\mu \phi_1 + \phi_2 \partial_\mu \phi_2)(\phi_1 \partial^\mu \phi_1 + \phi_2 \partial^\mu \phi_2)}{R^2 - \phi_1^2 - \phi_2^2} \simeq \frac{1}{R^2} \left( 1 + \frac{1}{R^2} (\phi_1^2 + \phi_2^2) + \frac{1}{R^4} (\phi_1^2 + \phi_2^2)^2 + \dots \right) \cdot (\phi_1 \partial_\mu \phi_1 + \phi_2 \partial_\mu \phi_2) (\phi_1 \partial^\mu \phi_1 + \phi_2 \partial^\mu \phi_2) ,$$

and  $\frac{1}{R^2}$  is a non-dimensional coupling constant, whereas the masses of the pseudo-Nambu-Goldstone bosons are respectively  $\lambda$  and  $\gamma$ .

Taking into account that in the natural system of units  $\hbar = c = 1$  the dimensions of fields, masses and coupling constants are  $[\phi_a] = 1 = [R]$ ,  $[\gamma] = M = [\lambda]$ , we define the non-dimensional space-time coordinates and masses

$$x^\mu \rightarrow \frac{x^\mu}{\lambda}, \quad \sigma^2 = \frac{\alpha_2^2 - \alpha_3^2}{\alpha_1^2 - \alpha_3^2} = \frac{\gamma^2}{\lambda^2}, \quad 0 < \sigma^2 \leq 1,$$

to write the action and the energy in terms of them:

$$S = \frac{1}{2} \int dt dx \left\{ \partial_\mu \phi_1 \partial^\mu \phi_1 + \partial_\mu \phi_2 \partial^\mu \phi_2 + \frac{(\phi_1 \partial_\mu \phi_1 + \phi_2 \partial_\mu \phi_2)(\phi_1 \partial^\mu \phi_1 + \phi_2 \partial^\mu \phi_2)}{R^2 - \phi_1^2 - \phi_2^2} - \phi_1^2(t, x) - \sigma^2 \cdot \phi_2^2(t, x) \right\} \quad (4)$$

$$E = \frac{\lambda}{2} \int dx \left\{ (\partial_t \phi_1)^2 + (\partial_t \phi_2)^2 + (\partial_x \phi_1)^2 + (\partial_x \phi_2)^2 + \frac{(\phi_1 \partial_t \phi_1 + \phi_2 \partial_t \phi_2)^2 + (\phi_1 \partial_x \phi_1 + \phi_2 \partial_x \phi_2)^2}{R^2 - \phi_1^2 - \phi_2^2} + \phi_1^2(t, x) + \sigma^2 \cdot \phi_2^2(t, x) \right\} .$$

In the time-independent homogeneous minima of the action or vacua of our model,  $\phi_1^{V^\pm} = \phi_2^{V^\pm} = 0$ ,  $\phi_3^{V^\pm} = \pm R$ , the North and South Poles, the  $\mathbb{Z}_2 \times \mathbb{Z}_2 \times \mathbb{Z}_2$ ,  $\phi_a \rightarrow (-1)^{\delta_{ab}} \phi_b$ ,  $b = 1, 2, 3$  symmetry of the action (1) is spontaneously broken to:  $\mathbb{Z}_2 \times \mathbb{Z}_2$ ,  $\phi_\alpha \rightarrow (-1)^{\delta_{\alpha\beta}} \phi_\beta$ ,  $\alpha, \beta = 1, 2$ . Finite energy configurations require:

$$\lim_{x \rightarrow \pm\infty} \frac{d\phi_\alpha}{dx} = 0 \quad , \quad \lim_{x \rightarrow \pm\infty} \phi_\alpha = 0 \quad . \quad (5)$$

Therefore, the configuration space  $\mathcal{C} = \{\text{Maps}(\mathbb{R}, \mathbb{S}^2) / E < +\infty\}$  is the union of four disconnected sectors  $\mathcal{C} = \mathcal{C}_{\text{NN}} \cup \mathcal{C}_{\text{SS}} \cup \mathcal{C}_{\text{NS}} \cup \mathcal{C}_{\text{SN}}$  labeled by the vacua reached by each configuration at the two disconnected components of the boundary of the real line.

### A. Spherical coordinates

We now solve the constraint by using spherical coordinates:  $\theta \in [0, \pi]$ ,  $\varphi \in [0, 2\pi]$

$$\begin{aligned}\phi_1(t, x) &= R \sin \theta(t, x) \cos \varphi(t, x) \\ \phi_2(t, x) &= R \sin \theta(t, x) \sin \varphi(t, x) \\ \phi_3(t, x) &= R \cos \theta(t, x) .\end{aligned}$$

In spherical coordinates the potential energy density (we shall denote in the sequel:  $\bar{\sigma} = \sqrt{1 - \sigma^2}$ ) is

$$V(\theta, \varphi) = \frac{R^2}{2} \sin^2 \theta (\sigma^2 + \bar{\sigma}^2 \cos^2 \varphi) \quad , \quad (6)$$

the action becomes

$$S = \int dt dx \left\{ \frac{R^2}{2} [\partial_\mu \theta \partial^\mu \theta + \sin^2 \theta \partial_\mu \varphi \partial^\mu \varphi] - \frac{R^2}{2} \sin^2 \theta (\sigma^2 + \bar{\sigma}^2 \cos^2 \varphi) \right\} \quad ,$$

and the field equations read:

$$\square \theta - \frac{1}{2} \sin 2\theta (\partial^\mu \varphi \partial_\mu \varphi - \cos^2 \varphi - \sigma^2 \sin^2 \varphi) = 0 \quad (7)$$

$$\partial^\mu (\sin^2 \theta \partial_\mu \varphi) - \frac{1}{2} \bar{\sigma}^2 \sin^2 \theta \sin 2\varphi = 0 . \quad (8)$$

Finite energy solutions for which the space-time dependence is of the form:

$$\theta(t, x) = \theta \left( \frac{x - vt}{\sqrt{1 - v^2}} \right), \quad \varphi(t, x) = \varphi \left( \frac{x - vt}{\sqrt{1 - v^2}} \right),$$

for some velocity  $v$ , are called solitary waves. Lorentz invariance allows us to obtain all the solitary waves in our model from solutions of the static field equations

$$\begin{aligned}\theta'' - \frac{1}{2} \sin 2\theta (\varphi')^2 &= \frac{1}{2} (\cos^2 \varphi + \sigma^2 \sin^2 \varphi) \sin 2\theta \quad (9) \\ \frac{d}{dx} (\sin^2 \theta \varphi') &= \frac{1}{2} \bar{\sigma}^2 \sin^2 \theta \sin 2\varphi \quad , \quad (10)\end{aligned}$$

where the notation is:  $\theta' = \frac{d\theta}{dx}$ ,  $\varphi' = \frac{d\varphi}{dx}$ . The energy of the static configurations is:

$$\begin{aligned}E[\theta, \phi] &= \lambda \int dx \mathcal{E}(\theta'(x), \varphi'(x), \theta(x), \varphi(x)) \quad , \\ \mathcal{E} &= \frac{\lambda R^2}{2} ((\theta')^2 + \sin^2 \theta (\varphi')^2 + \sin^2 \theta (\sigma^2 + \bar{\sigma}^2 \cos^2 \varphi)) .\end{aligned}$$

### III. TOPOLOGICAL KINKS

We start the search for solitary waves in this model by using the Rajaraman trial orbit method [17].

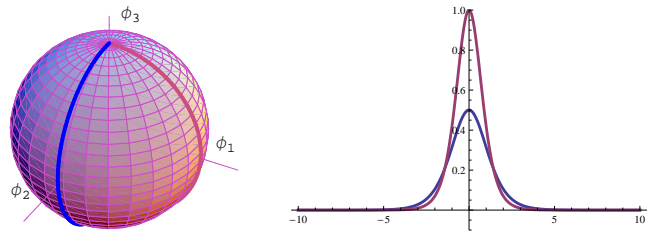


Figure 1: a)  $K_1$  and  $K_2$  ( $\sigma^2 = \frac{1}{2}$ ) kink orbits. b)  $K_1$  (blue) and  $K_2$  (red) kink energy densities

#### A. $K_1/K_1^*$ kinks

Our first trial orbit is:  $\varphi_{K_1}(x) = \frac{\pi}{2}$  or  $\varphi_{K_1^*}(x) = \frac{3\pi}{2}$ , i.e., the two halves of a single meridian, see Figure 1. The static field equations and the kink/antikink solutions are

$$\theta'' = \frac{\sigma^2}{2} \sin 2\theta \Rightarrow \theta_{K_1}(x) = \theta_{K_1^*}(x) = 2 \arctan e^{\pm \sigma(x-x_0)}$$

The energy of these kinks, which belong to  $\mathcal{C}_{\text{NS}}$  (kinks) or  $\mathcal{C}_{\text{SN}}$  (antikinks), is:

$$\begin{aligned}E_{K_1}^{\mathcal{C}} &= E_{K_1^*}^{\mathcal{C}} = \frac{\lambda R^2}{2} \int dx [(\theta'_{K_1})^2 + \sigma^2 \sin^2 \theta_{K_1}] = \\ &= \lambda R^2 \sigma^2 \int_{-\infty}^{\infty} \frac{dx}{\cosh^2 \sigma x} = 2\lambda R^2 \sigma .\end{aligned}$$

In the original field variables the  $K_1/K_1^*$  kink/ antikink solutions are:

$$\begin{aligned}\phi_1^{K_1}(x) &= \phi_1^{K_1^*}(x) = 0 \\ \phi_2^{K_1}(x) &= -\phi_2^{K_1^*}(x) = \frac{R}{\cosh[\sigma(x-x_0)]} \\ \phi_3^{K_1}(x) &= \phi_3^{K_1^*}(x) = \pm R \tanh[\sigma(x-x_0)].\end{aligned} \quad (11)$$

#### B. $K_2/K_2^*$ kinks

We now try the half-meridians  $\varphi_{K_2}(x) = 0$  or  $\varphi_{K_2^*}(x) = \pi$ . The static field equations and the kink/antikink solutions are:

$$\theta'' = \frac{1}{2} \sin 2\theta \Rightarrow \theta_{K_2}(x) = \theta_{K_2^*}(x) = 2 \arctan e^{\pm(x-x_0)}$$

The energy of the  $K_2/K_2^*$  kinks, which also belong to the  $\mathcal{C}_{\text{NS}}$ ,  $\mathcal{C}_{\text{SN}}$  sectors, is greater than the energy of the  $K_1/K_1^*$  kinks:

$$\begin{aligned}E_{K_2}^{\mathcal{C}} &= E_{K_2^*}^{\mathcal{C}} = \frac{\lambda R^2}{2} \int dx [(\theta'_{K_2})^2 + \sin^2 \theta_{K_2}] = \\ &= \lambda R^2 \int_{-\infty}^{\infty} \frac{dx}{\cosh^2 x} = 2\lambda R^2 .\end{aligned}$$

In the original field variables the kink/antikink  $K_2/K_2^*$  profiles are:

$$\begin{aligned}\phi_1^{K_2}(x) &= -\phi_1^{K_2^*}(x) = \frac{R}{\cosh(x-x_0)} \\ \phi_2^{K_2}(x) &= \phi_2^{K_2^*}(x) = 0 \\ \phi_3^{K_2}(x) &= \phi_3^{K_2^*}(x) = \pm R \tanh(x-x_0).\end{aligned}\quad (12)$$

### C. Degenerate families of $Q_\alpha$ -kinks

When  $\sigma^2 = 1$ , the system enjoys  $SO(2)$  internal symmetry and the masses of the two pseudo-Nambu-Goldstone bosons are equal, there are degenerate families of time-dependent  $Q$ -kinks of finite energy. If  $\sigma = 1$ ,

$$\varphi^{Q_\alpha}(t) = \omega t + \alpha,$$

where  $\omega$  and  $\alpha$  are real constants, solves (8) for any time-independent  $\theta(x)$ . Moreover, by plugging  $\varphi^{Q_\alpha}(t)$  into (7) one obtains:

$$\begin{aligned}-\theta'' + \frac{1}{2}(1-\omega^2)\sin 2\theta &= 0 \Rightarrow \\ \theta^{Q_\alpha}(x) &= 2 \arctan e^{\pm\sqrt{1-\omega^2}(x-x_0)}, \quad \forall \alpha.\end{aligned}\quad (13)$$

Therefore, if  $0 < \omega^2 < 1$ , the  $(\theta^{Q_\alpha}(x), \varphi^{Q_\alpha}(t))$  configurations form a degenerate circle of periodic in time  $Q$ -kink solutions of energy:

$$\begin{aligned}E_{Q_\alpha}^C &= \frac{\lambda R^2}{2} \int dx \left[ \left( \frac{d\theta^{Q_\alpha}}{dx} \right)^2 + (1+\omega^2) \sin^2 \theta^{Q_\alpha}(x) \right] \\ &= \frac{2\lambda R^2}{\sqrt{1-\omega^2}} = \frac{2\lambda R^2}{\bar{\omega}}, \quad \forall \alpha.\end{aligned}$$

In another reference frame moving with respect to the  $Q_\alpha$ -kink CM with velocity  $v$ , the interplay between  $x$  and  $t$  dependence is more complicated:

$$\begin{aligned}\varphi^{Q_\alpha}(x, t) &= \omega \left( \frac{t - vx}{\sqrt{1-v^2}} \right) + \alpha \\ \theta^{Q_\alpha}(x, t) &= 2 \arctan e^{\pm\bar{\omega} \left( \frac{x-vt}{\sqrt{1-v^2}} - x_0 \right)}.\end{aligned}$$

In Cartesian coordinates the  $Q_\alpha$ -kinks in the CM system are:

$$\begin{aligned}\phi_1^{Q_\alpha}(x, t) &= \frac{R \cos(\omega t + \alpha)}{\cosh[\bar{\omega}(x-x_0)]} \\ \phi_2^{Q_\alpha}(x, t) &= \frac{R \sin(\omega t + \alpha)}{\cosh[\bar{\omega}(x-x_0)]} \\ \phi_3^{Q_\alpha}(x, t) &= \pm R \tanh[\bar{\omega}(x-x_0)].\end{aligned}\quad (14)$$

At the  $\omega = 0$  limit we find a circle of static topological kinks that form a degenerate family of solitary waves of the system.

## IV. TOPOLOGICAL KINK STABILITY

### A. Small fluctuations on topological kinks

The analysis of small fluctuations around topological kinks requires us to consider both the geodesic deviation operator and the Hessian of the potential energy density. In order to set the geodesic deviations from the kink orbits, we rewrite the arc-length, the (non-null) Christoffel symbols and, the (non-null) components of the Curvature tensor in the geodesic coordinate system ( $\theta = \theta^1 \in [0, \partial]$ ),  $\varphi = \theta^2 \in [0, 2\pi]$ ):

$$\begin{aligned}ds^2 &= R^2 d\theta^1 d\theta^1 + R^2 \sin^2 \theta^1 d\theta^2 d\theta^2 \\ \Gamma_{22}^1 &= -\frac{1}{2} \sin 2\theta^1, \quad \Gamma_{12}^2 = \Gamma_{21}^2 = \cotan \theta^1 \\ R_{212}^1 &= -R_{122}^1 = \sin^2 \theta^1, \quad R_{121}^2 = -R_{211}^2 = 1.\end{aligned}$$

Note the mild change in notation. We also denote the Kink trajectories and small deformations around them as:  $\theta_K(x) = (\theta_K^1(x) = \bar{\theta}, \theta_K^2(x) = \bar{\varphi})$ ,  $\theta(x) = \theta_K(x) + \eta(x)$ ,  $\eta(x) = (\eta^1(x), \eta^2(x))$ .

Let us consider the following contra-variant vector fields along the kink trajectory,  $\eta, \theta'_K \in \Gamma(T\mathbb{S}^2|_K)$ :  $\eta(x) = \eta^1(x) \frac{\partial}{\partial \theta^1} + \eta^2(x) \frac{\partial}{\partial \theta^2}$  and  $\theta'_K(x) = \bar{\theta}'^i \frac{\partial}{\partial \theta^i} + \bar{\varphi}'^j \frac{\partial}{\partial \theta^j}$ .

The covariant derivative of  $\eta(x)$  and the action of the curvature tensor on  $\eta(x)$  are:

$$\begin{aligned}\nabla_{\theta'_K} \eta &= (\eta'^i(x) + \Gamma_{jk}^i \eta^j \bar{\theta}'^k) \frac{\partial}{\partial \theta^i} \\ R(\theta'_K, \eta) \theta'_K &= \bar{\theta}'^i \eta^j(x) \bar{\theta}'^k R_{ijk}^l \frac{\partial}{\partial \theta^l}.\end{aligned}$$

The geodesic deviation operator is:

$$\frac{D^2 \eta}{dx^2} + R(\theta'_K, \eta) \theta'_K = \nabla_{\theta'_K} \nabla_{\theta'_K} \eta + R(\theta'_K, \eta) \theta'_K.$$

To obtain the differential operator that governs the second-order fluctuations around the kink  $\theta_K$ , the remaining ingredient is the Hessian of the potential:

$$\nabla_\eta \text{grad} V = \eta^i \left( \frac{\partial^2 V}{\partial \theta^i \partial \theta^j} - \Gamma_{ij}^k \frac{\partial V}{\partial \theta^k} \right) g^{jl} \frac{\partial}{\partial \theta^l}$$

evaluated at  $\theta_K(x)$ . In sum, second-order kink fluctuations are determined by the operator:

$$\begin{aligned}\Delta_K \eta &= - \left[ \frac{D^2 \eta}{dx^2} + R(\theta'_K, \eta) \theta'_K + \nabla_\eta \text{grad} V \right] = \\ &= - \left( \frac{d^2 \eta^1}{dx^2} - \cos 2\bar{\theta} [\bar{\varphi}'^2 + \sigma^2 + \bar{\sigma}^2 \cos^2 \bar{\varphi}] \eta^1 - \sin 2\bar{\theta} \bar{\varphi}'^j \frac{d\eta^2}{dx} \right. \\ &= - \left[ (1 + \cos 2\bar{\theta}) \bar{\varphi}'^j \bar{\theta}'^j + \frac{\sin 2\bar{\theta}}{2} (\bar{\varphi}'' - \bar{\sigma}^2 \frac{\sin 2\bar{\varphi}}{2}) \right] \eta^2 \Big) \frac{\partial}{\partial \theta^1} \\ &= - \left( 2 \cotan \bar{\theta} \bar{\varphi}'^j \frac{d\eta^1}{dx} + (\cotan \bar{\theta} \bar{\varphi}'' - \bar{\varphi}'^j \bar{\theta}'^j) \eta^1 + \frac{d^2 \eta^2}{dx^2} + \right. \\ &= \left. 2 \cotan \bar{\theta} \bar{\theta}'^j \frac{d\eta^2}{dx} + (\cotan \bar{\theta} \bar{\theta}'' - \bar{\theta}'^2 - \cos^2 \bar{\theta} \bar{\varphi}'^2) \right) \frac{\partial}{\partial \theta^2} \quad (15)\end{aligned}$$

### B. The spectrum of small fluctuations around $K_1/K_1^*$ kinks

Plugging the  $K_1$  solutions into (15), we obtain the differential operator acting on the second-order fluctuation operator around the  $K_1/K_1^*$  kinks:

$$\Delta_{K_1}\eta = \Delta_{K_1^*}\eta = \left[ -\frac{d^2\eta^1}{dx^2} + \left( \sigma^2 - \frac{2\sigma^2}{\cosh^2\sigma x} \right) \eta^1 \right] \frac{\partial}{\partial\theta^1} + \left[ -\frac{d^2\eta^2}{dx^2} + 2\sigma\tanh\sigma x \frac{d\eta^2}{dx} + \bar{\sigma}^2\eta^2 \right] \frac{\partial}{\partial\theta^2}. \quad (16)$$

The vector fields  $v(x) = v^1(x)\frac{\partial}{\partial\theta^1} + v^2(x)\frac{\partial}{\partial\theta^2}$  parallel along the  $K_1/K_1^*$  kink orbits satisfy

$$\frac{dv^i}{dx} + \Gamma_{jk}^i \bar{\theta}^j v^k = 0 \quad \Rightarrow$$

$$\left\{ \begin{array}{l} \frac{dv^1}{dx} = 0, \quad v^1(x) = 1 \\ \frac{dv^2}{dx} + \sigma \frac{\cotan(2\arctan e^{\sigma x})}{\cosh\sigma x} v^2 = 0, \quad v^2(x) = \cosh\sigma x \end{array} \right. .$$

Therefore,  $v_1 = \frac{\partial}{\partial\theta^1}$ ,  $v_2(x) = \cosh\sigma x \frac{\partial}{\partial\theta^2}$  is a frame  $\{v_1, v_2\}$  in  $\Gamma(TS^2|_{K_1})$  parallel to the  $K_1$  kink orbit in which (16) reads:

$$\Delta_{K_1}\eta = \Delta_{K_1^*}\eta = \left[ -\frac{d^2\bar{\eta}^1}{dx^2} + \left( \sigma^2 - \frac{2\sigma^2}{\cosh^2\sigma x} \right) \bar{\eta}^1 \right] v_1 + \left[ -\frac{d^2\bar{\eta}^2}{dx^2} + \left( 1 - \frac{2\sigma^2}{\cosh^2\sigma x} \right) \bar{\eta}^2 \right] v_2, \quad (17)$$

where  $\eta = \bar{\eta}^1 v_1 + \bar{\eta}^2 v_2$ . Note that:  $\eta^1 = \bar{\eta}^1$ ,  $\eta^2 = \cosh\sigma x \bar{\eta}^2$ .

The second-order fluctuation operator (17) is a diagonal matrix of transparent Pösch-Teller Schrödinger operators with very well known spectra. In the  $v_1 = \frac{\partial}{\partial\theta^1}$  direction there is a bound state of zero eigenvalue and a continuous family of positive eigenfunctions:

$$\bar{\eta}_0^1(x) = \frac{1}{\cosh\sigma x}, \quad \varepsilon_0^{(1)} = 0 \\ \bar{\eta}_k^1(x) = e^{ik\sigma x} (\tanh\sigma x - ik), \quad \varepsilon^{(1)}(k) = \sigma^2(k^2 + 1).$$

In the  $v_2 = \cosh\sigma x \frac{\partial}{\partial\theta^2}$  direction the spectrum is similar but the bound state corresponds to a positive eigenvalue:

$$\bar{\eta}_{1-\sigma^2}^2(x) = \frac{1}{\cosh\sigma x}, \quad \varepsilon_{1-\sigma^2}^{(2)} = 1 - \sigma^2 > 0 \\ \bar{\eta}_k^2(x) = e^{ik\sigma x} (\tanh\sigma x - ik), \quad \varepsilon^{(2)}(k) = \sigma^2 k^2 + 1.$$

Because there are no fluctuations of negative eigenvalue, the  $K_1/K_1^*$  kinks are stable.

### C. One-loop shift to classical $K_1/K_1^*$ kink masses

The reflection coefficient of the scattering waves in the potential wells of the Schrödinger operators in (17) being zero, it is possible to use the Cahill-Comtet-Glauber

formula [2] (see also [18] for a more detailed derivation) to compute the quantum correction to the  $K_1$  classical kink mass up to one-loop order:

$$E_{K_1}(\sigma) = E_{K_1}^C(\sigma) + \Delta E_{K_1}(\sigma) + \mathcal{O}\left(\frac{1}{R^2}\right) = \\ = 2\lambda R^2 \sigma - \frac{\lambda\sigma}{\pi} \left[ \sin\nu_1 + \frac{1}{\sigma} \sin\nu_2 - \nu_1 \cos\nu_1 - \frac{1}{\sigma} \nu_2 \cos\nu_2 \right] + \mathcal{O}\left(\frac{1}{R^2}\right) \quad (18)$$

In (18) the angles  $\nu_1 = \arccos(0) = \frac{\pi}{2}$ ,  $\nu_2 = \arccos\bar{\sigma}$ , are determined from the eigenvalues of the bound states and the thresholds of the continuous spectra. This simple structure of the one-loop kink mass shift occurs only for transparent potentials. In our model, we find the elegant formula:

$$E_{K_1}(\sigma) = 2\lambda R^2 \sigma - \frac{\lambda\sigma}{\pi} \left[ 2 - \frac{\bar{\sigma}}{\sigma} \arccos(\bar{\sigma}) \right] + \mathcal{O}\left(\frac{1}{R^2}\right) \quad (19)$$

For instance, for  $\sigma = \frac{1}{2}$  we obtain a result similar to the mass shift of the  $\lambda\phi_2^4$ -kink:

$$E_{K_1}\left(\frac{1}{2}\right) = \lambda R^2 - \frac{3\lambda}{2\pi} \left( \frac{2}{3} - \frac{\pi}{6\sqrt{3}} \right) + \mathcal{O}\left(\frac{1}{R^2}\right)$$

As in the  $\lambda\phi_2^4$ -kink case, a zero mode and a bound eigenstate of eigenvalue  $\varepsilon_{\frac{3}{4}}^{(2)} = \frac{3}{4}$  contribute. The gaps between the bound state eigenvalues and the thresholds  $\varepsilon^{(1)}(0) = \sigma^2$ ,  $\varepsilon^{(2)}(0) = 1$  of the two branches of the continuous spectrum are the same in our model. The gaps, however, are different from the gaps in the  $\lambda\phi_2^4$  model between the eigenvalues of the two bound states and the threshold of the only branch of the continuous spectrum. Both features contribute to the slightly different result. The  $\sigma = 1$  symmetric case is more interesting. We find exactly twice the spectrum of the sine-Gordon kink: two zero modes and two gaps with respect to the thresholds of the continuous spectrum equal to one. No wonder that the one-loop mass shifts of the degenerate kinks is twice the one-loop correction of the sine-Gordon kink:

$$E_{K_\alpha}(1) = 2\lambda \left( R^2 - \frac{1}{\pi} \right) + \mathcal{O}\left(\frac{1}{R^2}\right), \quad \forall \alpha !.$$

Moreover, the quantum fluctuations do not break the  $SO(2)$ -symmetry and our result fits in perfectly well with the one-loop shift to the mass of the  $\mathcal{N} = (2, 2)$  SUSY  $\mathbb{C}P^1$  kink computed in [19] where the authors find twice the mass of the  $\mathcal{N} = 1$  SUSY sine-Gordon kink. A different derivation of formula (19) following the procedure of [20], see also [21], [22], will be published elsewhere.

#### D. The spectrum of small fluctuations around $K_2/K_2^*$ kinks

By inserting the  $K_2$  solutions in (15) the second-order fluctuation operator around the  $K_2/K_2^*$  kinks is found:

$$\begin{aligned} \Delta_{K_2}\eta = \Delta_{K_2^*}\eta &= \left[ -\frac{d^2\eta^1}{dx^2} + \left(1 - \frac{2}{\cosh^2 x}\right)\eta^1 \right] \frac{\partial}{\partial\theta^1} \\ &+ \left[ -\frac{d^2\eta^2}{dx^2} + 2\tanh x \frac{d\eta^2}{dx} - \bar{\sigma}^2\eta^2 \right] \frac{\partial}{\partial\theta^2}. \end{aligned} \quad (20)$$

The parallel vectors fields along the  $K_2/K_2^*$  kink orbits satisfy:

$$\begin{aligned} \frac{du^1}{dx} &= 0; \quad u^1(x) = 1 \\ \frac{du^2}{dx} + \frac{\cotan(2\arctan e^x)}{\cosh x} u^2 &= 0; \quad u^2(x) = \cosh x. \end{aligned}$$

In the parallel frame  $\{u_1, u_2\} \in \Gamma(T\mathbb{S}^2|_{K_2})$ ,  $u_1 = \frac{\partial}{\partial\theta^1}$ ,  $u_2(x) = \cosh x \frac{\partial}{\partial\theta^2}$ , to the  $K_2/K_2^*$  orbits (20) becomes:

$$\begin{aligned} \Delta_{K_2}\eta &= \Delta_{K_2^*}\eta = \left[ -\frac{d^2\tilde{\eta}^1}{dx^2} + \left(1 - \frac{2}{\cosh^2 x}\right)\tilde{\eta}^1 \right] u_1 \\ &+ \left[ -\frac{d^2\tilde{\eta}^2}{dx^2} + \left(\sigma^2 - \frac{2}{\cosh^2 x}\right)\tilde{\eta}^2 \right] u_2. \end{aligned} \quad (21)$$

with  $\eta = \tilde{\eta}^1 u_1 + \tilde{\eta}^2 u_2$ ,  $\eta^1 = \tilde{\eta}^1$ ,  $\eta^2 = \cosh x \tilde{\eta}^2$ .

Again, the second-order fluctuation operator (20) is a diagonal matrix of transparent Pösch-Teller operators. In this case, there is a bound state of zero eigenvalue and a continuous family of positive eigenfunctions starting at the threshold  $\varepsilon^{(1)}(0) = 1$  in the  $u_1 = \frac{\partial}{\partial\theta^1}$  direction:

$$\begin{aligned} \tilde{\eta}_0^1(x) &= \frac{1}{\cosh x}, \quad \varepsilon_0^{(1)} = 0 \\ \tilde{\eta}_k^1(x) &= e^{ikx}(\tanh x - ik), \quad \varepsilon^{(1)}(k) = (k^2 + 1). \end{aligned}$$

In the  $u_2(x) = \cosh x \frac{\partial}{\partial\theta^2}$  direction, the spectrum is similar but the eigenvalue of the bound state is negative, whereas the threshold of this branch of the continuous spectrum is  $\varepsilon^{(2)}(0) = \sigma^2$ :

$$\begin{aligned} \tilde{\eta}_{\sigma^2-1}^2(x) &= \frac{1}{\cosh x}, \quad \varepsilon_{\sigma^2-1}^{(2)} = \sigma^2 - 1 < 0 \\ \tilde{\eta}_k^2(x) &= e^{ikx}(\tanh x - ik), \quad \varepsilon^{(2)}(k) = k^2 + \sigma^2. \end{aligned}$$

Therefore,  $K_2/K_2^*$  kinks are unstable and a Jacobi field for  $k = i\sigma$  arises:  $\tilde{\eta}_J^2(x) = e^{\sigma x}(\tanh x - \sigma)$ ,  $\varepsilon_J^{(2)} = 0$ .

#### E. One-loop shift to classical $K_2/K_2^*$ kink masses

Once again we use the Cahill-Comtet-Glauber formula to compute the quantum correction to the  $K_2$  classical

kink mass up to one-loop order:

$$\begin{aligned} E_{K_2}(\sigma) &= E_{K_2}^C(\sigma) + \Delta E_{K_2}(\sigma) + \mathcal{O}\left(\frac{1}{R^2}\right) = \\ &= 2\lambda R^2 - \frac{\lambda\sigma}{\pi} \left[ \frac{1}{\sigma} \sin \nu_1 + \sin \nu_2 - \frac{1}{\sigma} \nu_1 \cos \nu_1 \right. \\ &\quad \left. - \nu_2 \cos \nu_2 \right] + \mathcal{O}\left(\frac{1}{R^2}\right). \end{aligned} \quad (22)$$

As before, the angles  $\nu_1 = \arccos(0) = \frac{\pi}{2}$ ,  $\nu_2 = \arccos(i\bar{\sigma})$ , are determined from the eigenvalues of the bound states and the thresholds of the continuous spectra. The novelty is that since the bound state eigenvalue is negative  $\nu_2$  is purely imaginary. Therefore, we find:

$$\begin{aligned} E_{K_2}(\sigma) &= 2\lambda R^2 - \frac{\lambda\sigma}{\pi} \left[ \frac{1}{\sigma} + \sqrt{2 - \sigma^2} - i\frac{\pi}{2}\bar{\sigma} \right. \\ &\quad \left. + \bar{\sigma} \log \left[ \sqrt{2 - \sigma^2} - \bar{\sigma} \right] \right] + \mathcal{O}\left(\frac{1}{R^2}\right). \end{aligned} \quad (23)$$

The key point is that the one-loop mass shift is a complex quantity, the imaginary part telling us about the life-time of this resonant state. For  $\sigma = \frac{1}{2}$ , the energy of the  $K_2$  kinks is:

$$\begin{aligned} E_{K_2}\left(\frac{1}{2}\right) &= 2\lambda R^2 - \frac{\lambda}{4\pi} \left( 4 + \sqrt{7} + \sqrt{3} \log \left[ \frac{\sqrt{7} - \sqrt{3}}{2} \right] \right. \\ &\quad \left. - i\pi \frac{\sqrt{3}}{2} \right) + \mathcal{O}\left(\frac{1}{R^2}\right). \end{aligned}$$

In the  $\sigma = 1$  symmetric case, however, we find the expected purely real answer:

$$E_{K_2}(1) = 2\lambda \left( R^2 - \frac{1}{\pi} \right) + \mathcal{O}\left(\frac{1}{R^2}\right).$$

#### V. BPS VERSUS NON-BPS TOPOLOGICAL KINKS

The different natures of the  $K_1$  and  $K_2$  kinks can be understood by relying on the ‘‘mechanical analogy’’: one thinks of the ODE system (9,10) as the Newton equations for the evolution of a particle in ‘‘time’’  $x$ , with  $(\theta, \varphi)$  ‘‘position’’ in the  $\mathbb{S}^2$ -sphere, moving in a ‘‘potential’’  $U(\theta, \varphi) = -V(\theta, \varphi)$ , see [23]. Thus, we are dealing with a famous integrable system -the Neumann problem [26]- although in our case the linear force is repulsive rather than attractive.

The four representations of the Hamilton characteristic function

$$\begin{aligned} W^{(\beta_1, \beta_2)}(\theta, \varphi) &= \\ &(-1)^{\beta_1} R^2 \sqrt{(1 + (-1)^{\beta_2} \sigma \cos \theta)^2 - \bar{\sigma}^2 \sin^2 \theta \cos^2 \varphi} \end{aligned}$$

$(\beta_1, \beta_2 = 0, 1)$  form a complete integral of the ‘‘time’’-independent Hamilton-Jacobi equation for zero ‘‘particle

energy”:

$$V(\theta, \varphi) = \frac{1}{2R^2} \left( \left( \partial_\theta W^{(\beta_1, \beta_2)} \right)^2 + \frac{1}{\sin^2 \theta} \left( \partial_\varphi W^{(\beta_1, \beta_2)} \right)^2 \right) \quad (24)$$

$\forall \beta_1, \beta_2$ . In terms of these, we write the static field energy (the particle “action”) á la Bogomolny [27]:

$$E(\theta, \varphi) = \frac{\lambda R^2}{2} \int dx \left[ \left( \theta' - \frac{1}{R^2} \partial_\theta W^{(\beta_1, \beta_2)} \right)^2 + \sin^2 \theta \left( \varphi' - \frac{1}{R^2 \sin^2 \theta} \partial_\varphi W^{(\beta_1, \beta_2)} \right)^2 \right] + \lambda \int dx \left\{ \theta' \partial_\theta W^{(\beta_1, \beta_2)} + \varphi' \partial_\varphi W^{(\beta_1, \beta_2)} \right\}$$

The solutions of the first-order equations:

$$\frac{d\theta}{dx} = \frac{1}{R^2} \frac{\partial W^{(\beta_1, \beta_2)}}{\partial \theta} = -(-1)^{\beta_1} \cdot \frac{\sigma \sin \theta \left( (-1)^{\beta_2} + \cos \theta (\sigma + \bar{\sigma}^2 \cos^2 \varphi) \right)}{\sqrt{\left( (-1)^{\beta_2} + \sigma \cos \theta \right)^2 - \bar{\sigma}^2 \sin^2 \theta \cos^2 \varphi}} \quad (25)$$

$$\frac{d\varphi}{dx} = \frac{1}{R^2 \sin^2 \theta} \frac{\partial W^{(\beta_1, \beta_2)}}{\partial \varphi} = (-1)^{\beta_1} \cdot \frac{\bar{\sigma} \cos \varphi \sin \varphi}{\sqrt{\left( (-1)^{\beta_2} + \sigma \cos \theta \right)^2 - \bar{\sigma}^2 \sin^2 \theta \cos^2 \varphi}} \quad (26)$$

are both solutions of (9,10) and absolute minima of  $E$  in each topological sector. The solutions of (25)-(26) are the flow lines induced by the gradient of  $W^{(\beta_1, \beta_2)}$ . There are two pairs of branching points in  $W^{(\beta_1, \beta_2)}$  (depending on the choice of  $\beta_2$ ), i.e.,  $\varphi_B = 0, \pi$ ;  $(1 + (-1)^{\beta_2} \sigma \cos \theta_B^\pm)^2 = \bar{\sigma}^2 \sin^2 \theta_B^\pm \Rightarrow \cos \theta_B^\pm = -(-1)^{\beta_2} \sigma \equiv \theta_B^\pm = (1 + (-1)^{\beta_2}) \frac{\pi}{2} \pm \arccos \sigma$ .

The gradient flow is undefined at these points and the interpretation of the orbits that solve (25)-(26) and pass through them is problematic.

### A. BPS $K_1$ topological kinks

The  $K_1/K_1^*$  orbits,  $\varphi_{K_1}/\varphi_{K_1^*} = \frac{\pi}{2}/\frac{3\pi}{2}$ , do not cross the branching points and everything is fine. In these orbits, the Hamilton's characteristic function and the first-order equations reduce to:  $W^{(\beta_1, \beta_2)}(\theta, \frac{\pi}{2}) = W^{(\beta_1, \beta_2)}(\theta, \frac{3\pi}{2}) = (-1)^{\beta_1} R^2 (1 + (-1)^{\beta_2} \sigma \cos \theta) \Rightarrow$

$$\frac{d\theta}{dx} = -(-1)^{\beta_1} \sigma \sin \theta. \quad (27)$$

Thus,  $K_1$  kinks solve (25)-(26) and their energy, depending only on the values of  $W^{(\beta_1, \beta_2)}$  at the orbit endpoints, is a topological bound:

$$E_{K_1}^C = E_{K_1^*}^C = \lambda \left| W^{(\beta_1, \beta_2)}(0, \pm \frac{\pi}{2}) - W^{(\beta_1, \beta_2)}(\pi, \pm \frac{\pi}{2}) \right| = 2\lambda R^2 \sigma^2.$$

We term these solitary waves BPS kinks even in this purely bosonic setting because they are bona fide solutions of the first-order equations and saturate the Bogomolny bound.

### B. Non-BPS $K_2$ topological kinks

The  $K_2/K_2^*$  orbits,  $\varphi_{K_2}/\varphi_{K_2^*} = 0/\pi$ , cross the branching points and things become more difficult. In these orbits the Hamilton characteristic functions are  $W^{(\beta_1, \beta_2)}(\theta, 0) = W^{(\beta_1, \beta_2)}(\theta, \pi) = (-1)^{\beta_1} R^2 ((-1)^{\beta_2} \sigma + \cos \theta)$ , whereas the first-order equations become:

$$\frac{d\theta}{dx} = -(-1)^{\beta_1} \sin \theta \cdot \frac{(-1)^{\beta_2} \sigma + \cos \theta}{|(-1)^{\beta_2} \sigma + \cos \theta|} \quad (28)$$

Note that we have not canceled the numerator against the denominator in (28) because for the  $K_2/K_2^*$  kink solutions there is a change of sign in the numerator after crossing the branching point:

$$\begin{aligned} \text{sign} \left( (-1)^{\beta_2} \sigma + \cos[2 \arctan e^{-x}] \right) &= \\ &= \begin{cases} + & \text{if } \cos[2 \arctan e^{-x}] > -(-1)^{\beta_2} \sigma \\ - & \text{if } \cos[2 \arctan e^{-x}] < -(-1)^{\beta_2} \sigma \end{cases} \end{aligned}$$

Thus, a solitary wave solution of the second order equations (9,10) like the  $K_2/K_2^*$  kinks with no change in the sign of  $\frac{d\theta}{dx}$  does not satisfy a unique first-order equation; these kinks are built by gluing together at the branching points one solution of the  $\beta_1 = 0$  (28) first-order ODE with one solution of the  $\beta_1 = 1$  (28) ODE:

$$\begin{aligned} \log \tan \left[ \frac{\theta}{2} \right] = -x &\Leftrightarrow \\ \Leftrightarrow \begin{cases} \beta_1 = 0 & \underline{\text{and}} & \text{sign} \left[ (-1)^{\beta_2} \sigma + \cos \theta \right] = + \\ \beta_1 = 1 & \underline{\text{and}} & \text{sign} \left[ (-1)^{\beta_2} \sigma + \cos \theta \right] = - \end{cases} \end{aligned}$$

The gluing points are:  $2 \arctan e^{-x_B} = \theta_B^\pm$ .

The BPS bound is not saturated because the Stokes theorem works piece-wise

$$\begin{aligned} E_{K_2}^C &= E_{K_2^*}^C = \\ &\lambda \left| W^{(\beta_1, \beta_2)}(0, 0) - W^{(\beta_1, \beta_2)}(\theta_B^-, 0) \right| \\ &+ \lambda \left| W^{(\beta_1, \beta_2)}(\theta_B^-, 0) - W^{(\beta_1, \beta_2)}(\pi, 0) \right| \\ &= \lambda R^2 |1 + (-1)^{\beta_2} \sigma| + \lambda R^2 |1 - (-1)^{\beta_2} \sigma| = 2\lambda R^2 \end{aligned}$$

and these kinks are not BPS.

### C. BPS $Q_\alpha$ -kinks as $d = 1 + 1$ dyons

In the  $\sigma^2 = 1$  case there is symmetry with respect to the  $\exp[\alpha \begin{pmatrix} 0 & -1 & 0 \\ 1 & 0 & 0 \\ 0 & 0 & 0 \end{pmatrix}] \in \mathbb{SO}(2)$  subgroup of the  $\mathbb{O}(3)$

group. The associated Nöether charge distinguishes between different  $Q_\alpha$ -kinks :

$$Q = \frac{1}{2} \int dx (\phi_1 \partial_t \phi_2 - \phi_2 \partial_t \phi_1) = R^2 \int dx \sin^2 \theta \partial_t \varphi$$

$$Q[Q_\alpha] = R^2 \omega \int dx \sin^2 \theta Q_\alpha = 2R^2 \frac{\omega}{\bar{\omega}} .$$

For configurations such that  $\theta$  is time-independent and  $\varphi$  is space-independent, it is possible to arrange the energy in the form:

$$E = \frac{\lambda R^2}{2} \int dx \{ \sin^2 \theta [\dot{\varphi} - \omega]^2 + [\theta' \pm \bar{\omega} \sin \theta]^2 \}$$

$$+ \lambda R^2 \int dx \{ \omega \sin^2 \theta \dot{\varphi} \mp \bar{\omega} \theta' \sin \theta \} , \quad (29)$$

( $\dot{\varphi} = \frac{d\varphi}{dt}(t)$ ), in such a way that the solutions of the first-order equations:

$$\dot{\varphi} = \omega \Rightarrow \varphi^{Q_\alpha}(t) = \omega t + \alpha$$

$$\theta' = \mp \bar{\omega} \sin \theta \Rightarrow \theta^{Q_\alpha}(x) = 2 \arctan e^{\mp \bar{\omega}(x-x_0)} ,$$

the  $Q_\alpha$ -kinks, saturate the Bogomolny bound and are BPS:

$$E_{\text{BPS}} = \frac{2\lambda R^2}{\bar{\omega}} = \lambda \{ \omega Q + \bar{\omega} T \} . \quad (30)$$

Here, the topological charge  $T = |W[\theta(+\infty, t)] - W[\theta(-\infty, t)]|$  coming from the superpotential  $W = R^2(1 \mp \cos \theta)$  valued at the  $Q_\alpha$ -kinks gives:  $T[Q_\alpha] = 2R^2, \forall \alpha$ . This explains why “one cannot dent a dyon” (even a one-dimensional cousin), see [24]. Conservation of the Nöether charge forbids the decay of  $Q_\alpha$  kinks, all of them living in the same topological sector, to others with less energy.

#### D. Bohr-Sommerfeld rule: $Q$ -kink energy and charge quantization

The Bohr-Sommerfeld quantization rule applied to periodic in time-classical solutions in our model reads:

$$\int_0^T dt \int dx \pi_\varphi(t, x) \frac{\partial \varphi}{\partial t}(t, x)$$

$$= R^2 \int_0^T dt \int dx \sin^2 \theta(x, t) \frac{\partial \varphi}{\partial t} \frac{\partial \varphi}{\partial t} = 2\pi n .$$

In [16] it is explained how derivation of this formula with respect to the period  $T = \frac{2\pi}{\omega}$  leads to the ODE:  $\lambda \frac{dn}{dE} = \omega^{-1}(E)$ , or,

$$\lambda \int_0^n dn = \int_{E_0}^{E_n} \frac{E dE}{\sqrt{E^2 - 4\lambda^2 R^4}} \quad (31)$$

in the  $Q$ -kink case. Integration of (31) gives:

$$\lambda n = \sqrt{E_n^2 - 4\lambda^2 R^4} - \sqrt{E_0^2 - 4\lambda^2 R^4} ,$$

equivalent to,

$$E_n = \lambda \sqrt{n^2 + 4R^4} , \quad (32)$$

starting from  $E_0 = 2\lambda R^2$  and assuming  $n$  to be a positive integer. The  $Q$ -kink energy is thus quantized and the frequencies and charges allowed by the Bohr-Sommerfeld rule form also a numerable infinite set:

$$\omega_n = \sqrt{1 - \frac{1}{1 + \frac{n^2}{4R^4}}} , \quad Q_n = n .$$

## VI. THE MASSIVE NON-LINEAR $\mathbb{S}^2$ -SIGMA MODEL IN SPHERICAL ELLIPTIC COORDINATES

The secret of this non-linear (1+1)-dimensional massive  $\mathbb{S}^2$ -sigma model is that its analogous mechanical system is Hamilton-Jacobi separable in spherical elliptic coordinates.

### A. The spherical elliptic system of orthogonal coordinates

The definition of elliptic coordinates in a sphere is as follows: one fixes two arbitrary points (and the pair of antipodal points) in  $\mathbb{S}^2$ . We choose these points with no loss of generality in the form:  $F_1 \equiv (\theta_f, \pi)$ ,  $F_2 \equiv (\theta_f, 0)$ ,  $\bar{F}_1 \equiv (\pi - \theta_f, 0)$ ,  $\bar{F}_2 \equiv (\pi - \theta_f, \pi)$ ,  $\theta_f \in (0, \frac{\pi}{2})$ .

The distance between the two fixed points is  $d = 2f = 2R\theta_f < \pi R$ , see Figure 2(a). Given a point  $P \in \mathbb{S}^2$ , let

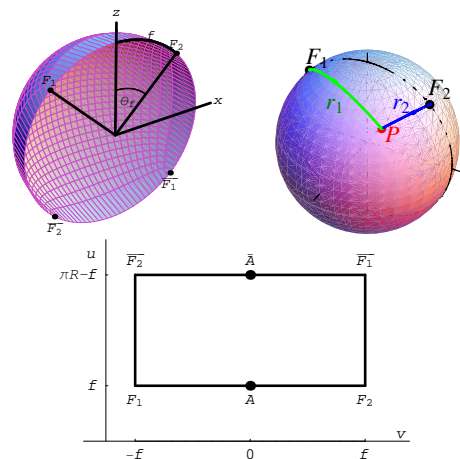


Figure 2: (a) Foci and antipodal foci of the elliptic system of coordinates on the sphere. (b) Distances from a point to the foci. (c) Elliptic coordinates on the sphere.

us consider the distances  $r_1 \in [0, \pi R]$  and  $r_2 \in [0, \pi R]$



from  $P$  to  $F_1$  and  $F_2$ .

$$r_1 = 2R \arcsin \sqrt{\frac{1}{2}(1 - \cos \theta_f \cos \theta + \sin \theta_f \sin \theta \cos \varphi)}$$

$$r_2 = 2R \arcsin \sqrt{\frac{1}{2}(1 - \cos \theta_f \cos \theta - \sin \theta_f \sin \theta \cos \varphi)},$$

see Figure 2(b). The spherical elliptic coordinates of  $P$  are half the sum and half the difference of  $r_1$  and  $r_2$ :

$$u = \frac{r_1 + r_2}{2}, v = \frac{r_1 - r_2}{2},$$

$u \in (R\theta_f, R(\pi - \theta_f))$ ,  $v \in (-R\theta_f, R\theta_f)$ , see Figure 2(c). We remark that this version of elliptic coordinates in a sphere is equivalent to using conical coordinates constrained to  $\mathbb{S}^2$ , as defined e. g. in Reference [25].

For simplicity, we shall use the abbreviated notation:

$$\text{su} = \sin \frac{u(t, x)}{R}, \text{sv} = \sin \frac{v(t, x)}{R}, \text{sf} = \sin \theta_f$$

$$\text{su}^2 = \sin^2 \frac{u(t, x)}{R}, \text{sv}^2 = \sin^2 \frac{v(t, x)}{R}, \text{sf}^2 = \sin^2 \theta_f$$

and analogously for  $\text{cu}$ ,  $\text{cv}$ , and  $\text{cf}$ . To pass from elliptical to Cartesian coordinates, or viceversa, one uses:

$$\phi_1(t, x) = \frac{R}{\text{sf}} \text{su sv}$$

$$\phi_2(t, x) = \pm \frac{R}{\text{sf cf}} \sqrt{(\text{su}^2 - \text{sf}^2)(\text{sf}^2 - \text{sv}^2)}$$

$$\phi_3(t, x) = \frac{R}{\text{cf}} \text{cu cv},$$

whereas the differential arc-length in elliptic coordinates reads:

$$ds_{\mathbb{S}^2}^2 = \frac{\text{su}^2 - \text{sv}^2}{\text{su}^2 - \text{sf}^2} \cdot du^2 + \frac{\text{su}^2 - \text{sv}^2}{\text{sf}^2 - \text{sv}^2} \cdot dv^2.$$

The spherical elliptic coordinates of the North and South Poles, and the foci are respectively:  $(u_N, v_N) = (R\theta_f, 0)$ ,  $(u_S, v_S) = (R(\pi - \theta_f), 0)$ ,  $(u_{F_1}, v_{F_1}) \equiv (R\theta_f, -R\theta_f)$ ,  $(u_{F_2}, v_{F_2}) \equiv (R\theta_f, R\theta_f)$ ,  $(u_{\bar{F}_1}, v_{\bar{F}_1}) \equiv (R(\pi - \theta_f), R\theta_f)$ ,  $(u_{\bar{F}_2}, v_{\bar{F}_2}) \equiv (R(\pi - \theta_f), -R\theta_f)$ .

### B. Static field equations and Hamilton-Jacobi separability

We choose a system of spherical elliptic coordinates with the foci determined by  $\theta_f = \arccos \sigma$ , i.e.,  $\sigma^2 = \cos^2 \theta_f$ ,  $\bar{\sigma}^2 = \sin^2 \theta_f$ . We stress that the foci (and their antipodal points) are the branching points mentioned in the previous Section. In this coordinate system the action for the massive non-linear  $\mathbb{S}^2$ -sigma model reads:

$$S = \int dt dx \left\{ \frac{1}{2} \left[ \frac{\text{su}^2 - \text{sv}^2}{\text{su}^2 - \text{sf}^2} \partial_\mu u \partial^\mu u + \frac{\text{su}^2 - \text{sv}^2}{\text{sf}^2 - \text{sv}^2} \partial_\mu v \partial^\mu v \right] - V(u(t, x), v(t, x)) \right\},$$

where:

$$V(u, v) = \frac{R^2}{2(\text{su}^2 - \text{sv}^2)} [\text{su}^2(\text{su}^2 - \text{sf}^2) + \text{sv}^2(\text{sf}^2 - \text{sv}^2)].$$

The field equations are:

$$\partial_\mu \left( \frac{\text{su}^2 - \text{sv}^2}{\text{su}^2 - \text{sf}^2} \cdot \partial^\mu u \right) = -\frac{\delta V}{\delta u}$$

$$\partial_\mu \left( \frac{\text{su}^2 - \text{sv}^2}{\text{sf}^2 - \text{sv}^2} \cdot \partial^\mu v \right) = -\frac{\delta V}{\delta v}$$

whereas the static energy reads:

$$E[u, v] = \lambda \int dx \mathcal{E}(u'(x), v'(x), u(x), v(x)),$$

$$\mathcal{E} = \frac{1}{2} \left[ \frac{\text{su}^2 - \text{sv}^2}{\text{su}^2 - \text{sf}^2} (u')^2 + \frac{\text{su}^2 - \text{sv}^2}{\text{sf}^2 - \text{sv}^2} (v')^2 \right] + V(u, v).$$

Let us think of  $E[u, v]$  as the action for a particle:  $\mathcal{E}$  as the Lagrangian,  $x$  as the time,  $U(u, v) = -V(u, v)$  as the mechanical potential energy, and the target manifold  $\mathbb{S}^2$  as the configuration space. The canonical momenta are:

$$p_u = \frac{\partial \mathcal{E}}{\partial u'} = \frac{\text{su}^2 - \text{sv}^2}{\text{su}^2 - \text{sf}^2} u', p_v = \frac{\partial \mathcal{E}}{\partial v'} = \frac{\text{su}^2 - \text{sv}^2}{\text{sf}^2 - \text{sv}^2} v',$$

and the static field equations can be thought of as the Newtonian ODE's:

$$\frac{d}{dx} \cdot \left( \frac{\text{su}^2 - \text{sv}^2}{\text{su}^2 - \text{sf}^2} \cdot u' \right) = \frac{\delta V}{\delta u}$$

$$\frac{d}{dx} \cdot \left( \frac{\text{su}^2 - \text{sv}^2}{\text{sf}^2 - \text{sv}^2} \cdot v' \right) = \frac{\delta V}{\delta v}.$$

Because the mechanical energy is

$$U(u, v) = -V(u, v) = -\frac{1}{\text{su}^2 - \text{sv}^2} (f(u) + g(v)) =$$

$$= -\frac{R^2 [\text{su}^2(\text{su}^2 - \text{sf}^2) + \text{sv}^2(\text{sf}^2 - \text{sv}^2)]}{2(\text{su}^2 - \text{sv}^2)}$$

this mechanical system is a Liouville type I integrable system, (see [28] to find the classification of two dimensional integrable systems of Liouville type.) The Hamiltonian and the Hamilton-Jacobi equation of spherical Type I Liouville models have the form:

$$H = \frac{h_u + h_v}{\text{su}^2 - \text{sv}^2}, \begin{cases} h_u = \frac{1}{2}(\text{su}^2 - \text{sf}^2) p_u^2 - f(u) \\ h_v = \frac{1}{2}(\text{sf}^2 - \text{sv}^2) p_v^2 - g(v) \end{cases}$$

$$\frac{\partial \mathcal{S}}{\partial x} + H \left( \frac{\partial \mathcal{S}}{\partial u}, \frac{\partial \mathcal{S}}{\partial v}, u, v \right) = 0,$$

which guarantees Hamilton-Jacobi separability in this system of coordinates. The separation ansatz  $\mathcal{S}(x, u, v) = -i_1 x + \mathcal{S}_u(u) + \mathcal{S}_v(v)$  reduces the Hamilton-Jacobi equation to the two separated ODE's:

$$\frac{i_2}{R^2} = i_1 \text{su}^2 - \frac{1}{2}(\text{su}^2 - \text{sf}^2) \left( \frac{d\mathcal{S}_u}{du} \right)^2 + f(u)$$

$$\frac{i_2}{R^2} = i_1 \text{sv}^2 + \frac{1}{2}(\text{sf}^2 - \text{sv}^2) \left( \frac{d\mathcal{S}_v}{dv} \right)^2 - g(v),$$

which can be easily integrated to find the complete solution  $\mathcal{S} = \mathcal{S}(x, u, v, i_1, i_2)$  of the HJ equation:

$$\begin{aligned} \mathcal{S} = & -i_1 x + \text{sg}(p_u) \int du \sqrt{\frac{2(\frac{i_2}{R^2} + i_1 su^2 + f(u))}{su^2 - sf^2}} \\ & + \text{sg}(p_v) \int dv \sqrt{\frac{2(-\frac{i_2}{R^2} - i_1 sv^2 + g(v))}{sf^2 - sv^2}} \end{aligned} \quad (33)$$

in terms of the mechanical energy  $I_1 = i_1$  and a second constant of motion: the separation constant  $I_2 = \frac{i_2}{R^2}$ .

## VII. NON-TOPOLOGICAL KINKS

We now identify the families of trajectories corresponding to the values  $i_1 = i_2 = 0$  of the two invariants in the mechanical system. These orbits are separatrices between bounded and unbounded motion in phase space and become solitary wave solutions in the field-theoretical model because the  $i_1 = i_2 = 0$  conditions force the boundary behavior (5). (See [29] and [30] for application of this idea to the search for solitary waves in other two-scalar field models with analogous mechanical systems which are HJ separable in elliptic coordinates.)

1. In a first step we find the Hamilton characteristic function for zero particle energy ( $i_1 = 0 = i_2$ ) by performing the integrations in (33):

$$\begin{aligned} W^{(\beta_1, \beta_2)}(u, v) &= \mathcal{S}_u(u, i_1 = 0, i_2 = 0) \\ &+ \mathcal{S}_v(v, i_1 = 0, i_2 = 0) \\ &= F^{(\beta_1)}(u) + G^{(\beta_2)}(v) \end{aligned}$$

with  $(-1)^{\beta_1} = -\text{sg } p_u$ ,  $(-1)^{\beta_2} = -\text{sg } p_v \cdot \text{sg } v$ , and:

$$\begin{aligned} F^{(\beta_1)}(u) &= R^2 (-1)^{\beta_1} \cos \frac{u}{R} \\ G^{(\beta_2)}(v) &= R^2 (-1)^{\beta_2} \cos \frac{v}{R} . \end{aligned}$$

2. The Hamilton-Jacobi procedure now provides the kink orbits by integrating  $\text{sg } p_u \int \frac{du}{(su^2 - sf^2)|su|} - \text{sg } p_v \int \frac{dv}{(sf^2 - sv^2)|sv|} = R^3 \gamma_2$ :

$$e^{R^2 \gamma_2 sf^2} = \left[ \frac{\left| \tan \frac{u-f}{2R} \tan \frac{u+f}{2R} \right|^{\frac{1}{2cf}}}{\left| \tan \frac{u}{2R} \right|} \right]^{\text{sg } p_u} \cdot \left[ \frac{\left| \tan \frac{v}{2R} \right|}{\left| \tan \frac{v-f}{2R} \tan \frac{v+f}{2R} \right|^{\frac{1}{2cf}}} \right]^{\text{sg } p_v} . \quad (34)$$

In Figure 3(a) a Mathematica plot is offered showing several orbits complying with (34) for several values of the

integration constant  $\gamma_2$ . Note that all the orbits start and end at the North Pole and pass through the foci  $\bar{F}_1$  such that we have shown a one-parametric family of non-topological kink orbits. In fact, there are four families of non-topological kinks among the solutions of (34): the orbits of a second family also start and end at the North Pole but pass through  $\bar{F}_2$ . The orbits in the second pair of NTK families start and end at the South Pole and pass through either  $F_1$  or  $F_2$ .

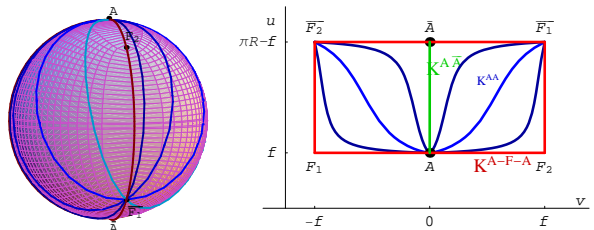


Figure 3: a) Several NTK kink orbits. b) The same NTK kink orbits in the elliptic rectangle.

3. The Hamilton-Jacobi procedure requires similar integrations in  $\text{sg } p_u \int \frac{|su| du}{(su^2 - sf^2)} - \text{sg } p_v \int \frac{|sv| dv}{(sf^2 - sv^2)} = R(x + \gamma_1)$  to find the kink profiles (or particle “time” schedules):

$$e^{2(x+\gamma_1)cf} = \frac{\left| \tan \frac{u(x)-f}{2R} \tan \frac{u(x)+f}{2R} \right|^{\text{sg } p_u}}{\left| \tan \frac{v(x)-f}{2R} \tan \frac{v(x)+f}{2R} \right|^{\text{sg } p_v}} . \quad (35)$$

In Figure 4 the NTK energy densities for three values of  $\gamma_2$  are plotted.

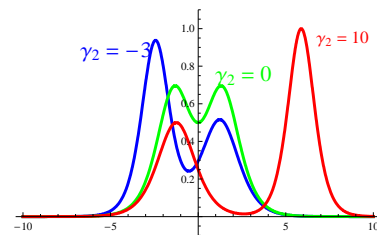


Figure 4: NTK energy densities for three different values of  $\gamma_2$ : 1)  $\gamma_2 = -3$ , highest peak on the left (blue) 2)  $\gamma_2 = 0$ , symmetrical peaks (green) 3)  $\gamma_2 = 10$  highest peak on the right (red).

4. Reshuffling equations (34) and (35), it is possible to find the two NTK families analytically, respectively based on  $(u_N, v_N) = (R\theta_f, 0)$  and  $(u_S, v_S) = (R(\pi - \theta_f), 0)$ :

$$\begin{aligned}\tan \frac{u_K(x, \gamma_1, \gamma_2)}{2R} &= \frac{\pm \sqrt{2\sqrt{1+e_1}e_2} t_{\frac{f}{2}}}{\sqrt{e_1 + e_2^2 + t_{\frac{f}{2}}^4 + e_1 e_2^2 t_{\frac{f}{2}}^4} - \sqrt{(e_1 + e_2^2 + t_{\frac{f}{2}}^4 + e_1 e_2^2 t_{\frac{f}{2}}^4)^2 - 4(1+e_1)^2 e_2^2 t_{\frac{f}{2}}^4}} \\ \tan \frac{v_K(x, \gamma_1, \gamma_2)}{2R} &= \frac{\pm \sqrt{e_1 + e_2^2 + t_{\frac{f}{2}}^4 + e_1 e_2^2 t_{\frac{f}{2}}^4} - \sqrt{(e_1 + e_2^2 + t_{\frac{f}{2}}^4 + e_1 e_2^2 t_{\frac{f}{2}}^4)^2 - 4(1+e_1)^2 e_2^2 t_{\frac{f}{2}}^4}}{\sqrt{2\sqrt{1+e_1}e_2} t_{\frac{f}{2}}}\end{aligned}\quad (36)$$

$$\begin{aligned}\tan \frac{u_K(x, \gamma_1, \gamma_2)}{2R} &= \frac{\pm \sqrt{e_1 + e_2^2 + t_{\frac{f}{2}}^4 + e_1 e_2^2 t_{\frac{f}{2}}^4} + \sqrt{(e_1 + e_2^2 + t_{\frac{f}{2}}^4 + e_1 e_2^2 t_{\frac{f}{2}}^4)^2 - 4(1+e_1)^2 e_2^2 t_{\frac{f}{2}}^4}}{\sqrt{2\sqrt{1+e_1}e_2} t_{\frac{f}{2}}} \\ \tan \frac{v_K(x, \gamma_1, \gamma_2)}{2R} &= \frac{\pm \sqrt{e_1 + e_2^2 + t_{\frac{f}{2}}^4 + e_1 e_2^2 t_{\frac{f}{2}}^4} + \sqrt{(e_1 + e_2^2 + t_{\frac{f}{2}}^4 + e_1 e_2^2 t_{\frac{f}{2}}^4)^2 - 4(1+e_1)^2 e_2^2 t_{\frac{f}{2}}^4}}{\sqrt{2\sqrt{1+e_1}e_2} t_{\frac{f}{2}}}\end{aligned}\quad (37)$$

where we have used the new abbreviations:  $e_1 = e^{2(x+\gamma_1)cf}$ ,  $e_2 = e^{x+\gamma_1-R^2\gamma_2 sf^2}$ ,  $t_{\frac{f}{2}} = \tan \frac{f}{2R}$ .

### VIII. NON-TOPOLOGICAL KINK INSTABILITY: MORSE INDEX THEOREM

To study the (lack of) stability of NTK kinks, it is convenient to use the following notation for the elliptic variables:  $u^1 = u$ ,  $u^2 = v$ . The static field equations read:

$$\frac{D}{dx} \cdot \frac{du^i}{dx} = g^{ij} \frac{d}{dx} \left( g_{jk} \frac{du^k}{dx} \right) = g^{ij} \frac{\partial V}{\partial u^j}. \quad (38)$$

Let us consider a one-parametric family of solutions of (38):  $u_K^i(x; \gamma)$ . The derivation of

$$\left( -\frac{D}{dx} \cdot \frac{du_K^i}{dx} + g^{ij}(u_K^1, u_K^2) \frac{\partial V}{\partial u^j} \right) \cdot g_{ik} \frac{\partial u_K^k}{\partial \gamma} = 0$$

with respect to the parameter  $\gamma$  implies:

$$\begin{aligned}\frac{D^2}{dx^2} \cdot \frac{\partial u_K^i}{\partial \gamma} + \frac{\partial u_K^j}{\partial x} \cdot \frac{\partial u_K^k}{\partial \gamma} \cdot \frac{\partial u_K^l}{\partial x} R_{jkl}^i + \\ + g^{ik} \left( \frac{\partial^2 V}{\partial u^j \partial u^k} - \Gamma_{jk}^l(u_K^1, u_K^2) \frac{\partial V}{\partial u^l} \right) \frac{\partial u_K^j}{\partial \gamma} = 0.\end{aligned}$$

In the last three formulas the metric tensor, the covariant derivatives, the connection, the curvature tensor, and the gradient and Hessian of the potential are valued on  $(u_K^1, u_K^2)$ , see [39]. Thus,  $\frac{\partial u_K^i}{\partial \gamma}$  is an eigenvector of the second order fluctuation operator of zero eigenvalue. The derivatives of the NTK solutions (36)/(37) with respect to the parameter  $\gamma_2$  are accordingly eigenvectors of the second order fluctuation operator of zero eigenvalues orthogonal to the NTK orbit, i.e., Jacobi fields that move from one NTK kink to another with no cost in energy.

Obtaining the explicit Jacobi fields using this idea is, however, extremely subtle. We first write (34) and (35)

in a new form:

$$\begin{aligned}e^{2R^2 sf^2 \gamma_2} &= \left( \frac{1+cu}{1-cu} \right)^{\text{sg}(p_u)} \left( \frac{1+cv}{1-cv} \right)^{\text{sg}(p_v)\text{sg}v} \\ &\cdot \left[ \left( \frac{cf-cu}{cf+cu} \right)^{\text{sg}(p_u)} \left( \frac{cv-cf}{cv+cf} \right)^{\text{sg}(p_v)\text{sg}v} \right]^{\frac{1}{cf}}\end{aligned}\quad (39)$$

$$e^{2cf(x+\gamma_1)} = \left( \frac{cf-cu}{cf+cu} \right)^{\text{sg}(p_u)} \left( \frac{cv-cf}{cv+cf} \right)^{\text{sg}(p_v)\text{sg}v} \quad (40)$$

The moduli space of NTK kinks described in (39)-(40) is formed by four disconnected sets. We choose one of these connected pieces to perform our analysis because the argument is identical in any of the four connected pieces. Thus, we shall focus on the  $v \geq 0$  semi-sphere,  $\phi_1 \geq 0$ , and on the family of NTKs “starting” and “finishing” at the South Pole  $\bar{A}$ . Each kink orbit in this family crosses the  $F_2$   $-(u, v) = (f, f)$ - focus. This behavior is achieved by the choice of  $\text{sg}(p_u) \neq \text{sg}(p_v)$  in the system of equations (39), (40).

The most difficult task is the identification of the  $x_0$  “instant” when a given NTK trajectory arrives at the  $F_2$  focus. Taking the limit  $u \rightarrow f+$  (from the right) and  $v \rightarrow f-$  (from the left) in equations (39) and (40), we find:

$$\begin{aligned}e^{2R^2 sf^2 \gamma_2} &= \lim_{(u,v) \rightarrow (f+, f-)} \left( \frac{cf-cu}{cv-cf} \right)^{\frac{\text{sg}(p_u)}{cf}} \\ e^{2(x_0+\gamma_1)} &= \lim_{(u,v) \rightarrow (f+, f-)} \left( \frac{cf-cu}{cv-cf} \right)^{\frac{\text{sg}(p_u)}{cf}}.\end{aligned}$$

Therefore,  $x_0 = -\gamma_1 + R^2 sf^2 \gamma_2$  is the arrival “time” in  $F_2$  which is different for the different NTK “trajectories” characterized by  $\gamma_2$ . This suggests the use of a new parameter,  $\tilde{\gamma}_1 = \gamma_1 - R^2 sf^2 \gamma_2$ , in such a way that all the NTKs “arrive” in  $F_2$  at the same “time”:  $x_0 = -\tilde{\gamma}_1$ .

With the help of (39), equation (40) is replaced in terms of the new parameter by:

$$e^{-2(x+\bar{\gamma}_1)} = \left( \frac{1+cu}{1-cu} \right)^{\text{sg}(p_u)} \left( \frac{1+cv}{1-cv} \right)^{\text{sg}(p_v)}. \quad (41)$$

Use of (41) allows us to re-write (39) in the new form:

$$e^{2R^2 \text{sf}^2 \gamma_2 + 2 \text{cf}(x+\bar{\gamma}_1)} = \left( \frac{\text{cf}-\text{cu}}{\text{cf}+\text{cu}} \right)^{\text{sg}(p_u)} \left( \frac{\text{cv}-\text{cf}}{\text{cv}+\text{cf}} \right)^{\text{sg}(p_v)} \quad (42)$$

With this re-shuffling of the equations, we ensure that all the NTK trajectories that solve (41)-(42) cross the  $F_2$  focus at the same “instant”:  $x_0 = -\bar{\gamma}_1$ . Implicit derivation with respect to  $\gamma_2$  of (41)-(42) provides the following linear system in the variables  $\frac{\partial u_K}{\partial \gamma_2}$ ,  $\frac{\partial v_K}{\partial \gamma_2}$ :

$$R^3 \text{sf}^2 = \frac{\text{sg}(p_u) \text{su}}{\text{su}^2 - \text{sf}^2} \frac{\partial u_K}{\partial \gamma_2} - \frac{\text{sg}(p_v) \text{sv}}{\text{sf}^2 - \text{sv}^2} \frac{\partial v_K}{\partial \gamma_2} \quad (43)$$

$$0 = \text{sg}(p_u) \text{sv} \frac{\partial u_K}{\partial \gamma_2} + \text{sg}(p_v) \text{su} \frac{\partial v_K}{\partial \gamma_2}. \quad (44)$$

Finally, we obtain the family of Jacobi fields:

$$J^{\text{NTK}}(x; \gamma_2) = \frac{R^3 (\text{su}^2 - \text{sf}^2) (\text{sf}^2 - \text{sv}^2)}{\text{su}^2 - \text{sv}^2} \cdot \left( \text{sg}(p_u) \text{su} \frac{\partial}{\partial u} - \text{sg}(p_v) \text{sv} \frac{\partial}{\partial v} \right). \quad (45)$$

In Figures 5 a)-b), 6 a)-b) two Jacobi fields for two values of  $\gamma_2$ , as well as the corresponding NTK field profiles, are plotted for the three  $\phi_1$ ,  $\phi_2$ ,  $\phi_3$  original field components.

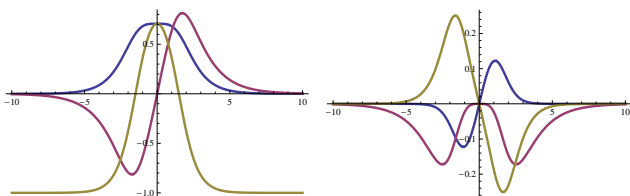


Figure 5: a) Profiles of the field components for NTK  $\gamma_2 = 0$  kink. b) Plot of the Jacobi field  $J^{\text{NTK}}(x; 0)$

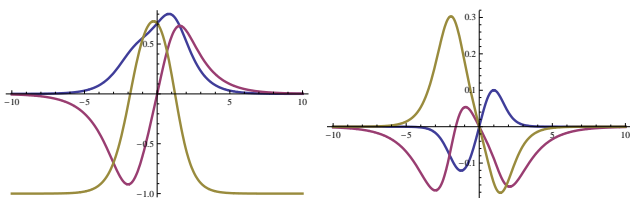


Figure 6: a) Profiles of the field components for NTK  $\gamma_2 = 1$  kink. b) Plot of the Jacobi field  $J^{\text{NTK}}(x; 1)$

The zeroes of the Jacobi fields along a given  $\gamma_2$ -NTK orbit (in the four disconnected sectors) are as follows: either  $A \equiv (u_K(-\infty; \gamma_2) = f, v_K(-\infty; \gamma_2) =$

$0)$ ,  $\bar{F}_1 \equiv (u_K(\bar{\gamma}_1; \gamma_2) = \pi R - f, v_K(\bar{\gamma}_1; \gamma_2) = -f)$ ,  $\bar{F}_2 \equiv (u_K(\bar{\gamma}_1; \gamma_2) = \pi R - f, v_K(\bar{\gamma}_1; \gamma_2) = f)$ , or,  $\bar{A} \equiv (u_K(-\infty; \gamma_2) = \pi R - f, v_K(-\infty; \gamma_2) = 0)$ ,  $F_1 \equiv (u_K(\bar{\gamma}_1; \gamma_2) = f, v_K(\bar{\gamma}_1; \gamma_2) = -f)$ ,  $F_2 \equiv (u_K(\bar{\gamma}_1; \gamma_2) = f, v_K(\bar{\gamma}_1; \gamma_2) = f)$ . Thus, the conjugate points with respect to either the North or the South Poles along the NTK orbits are listed below:

Starting Point	Conjugate Point	Conjugate Point
North Pole : $A$	Antipodal Focus : $\bar{F}_1$	Antipodal Focus : $\bar{F}_2$
South Pole : $\bar{A}$	Focus : $F_1$	Focus : $F_2$

In this two-dimensional setting, the Morse index theorem states that the number of negative eigenvalues of the second order fluctuation operator around a given orbit is equal to the number of conjugate points crossed by the orbit [31]. The reason is that the spectrum of the Schrödinger operator has in this case an eigenfunction with as many nodes as the Morse index, the Jacobi field, whereas the ground state has no nodes. The Jacobi fields of the NTK orbits cross one conjugate point, their Morse index is one, and the NTK kinks are unstable.

## IX. NON-BPS NON-TOPOLOGICAL KINKS

The availability of the Hamilton characteristic function as a sum of one function of  $u$  and another function of  $v$  allows us to write the energy of static configurations à la Bogomolny:

$$E[u, v] = \frac{\lambda}{2} \int dx \left\{ \frac{\text{su}^2 - \text{sv}^2}{\text{su}^2 - \text{sf}^2} \left( \frac{du}{dx} - \frac{\text{su}^2 - \text{sf}^2}{\text{su}^2 - \text{sv}^2} \frac{dF^{(\beta_1)}}{du} \right)^2 + \frac{\text{su}^2 - \text{sv}^2}{\text{sf}^2 - \text{sv}^2} \left( \frac{dv}{dx} - \frac{\text{sf}^2 - \text{sv}^2}{\text{su}^2 - \text{sv}^2} \frac{dG^{(\beta_2)}}{dv} \right)^2 \right\} + \lambda \int dx \frac{du}{dx} \frac{dF^{(\beta_1)}}{du} + \lambda \int dx \frac{dv}{dx} \frac{dG^{(\beta_2)}}{dv}.$$

Solutions of the first-order equations

$$\frac{du}{dx} = \frac{\text{su}^2 - \text{sf}^2}{\text{su}^2 - \text{sv}^2} \frac{dF^{(\beta_1)}}{du} = -R(-1)^{\beta_1} \frac{\text{su}^2 - \text{sf}^2}{\text{su}^2 - \text{sv}^2} \text{su} \quad (46)$$

$$\frac{dv}{dx} = \frac{\text{sf}^2 - \text{sv}^2}{\text{su}^2 - \text{sv}^2} \frac{dG^{(\beta_2)}}{dv} = -R(-1)^{\beta_2} \frac{\text{sf}^2 - \text{sv}^2}{\text{su}^2 - \text{sv}^2} \text{sv} \quad (47)$$

are absolute minima of the energy and therefore are stable. Note that the energy of the solutions of (46)-(47) is positive or zero because  $\text{sg}u' = \text{sg} \frac{dF^{(\beta_1)}}{du}$  and  $\text{sg}v' = \text{sg} \frac{dG^{(\beta_2)}}{dv}$ .

Even though the NTK trajectories are solutions of the analogous mechanical system provided by the HJ procedure that is closely related to the ODE system (46)-(47), they do not strictly solve (46)-(47). Taking the quotient

of the two equations in (46)-(47) we find the equation

$$\frac{du}{dv} = (-1)^{\beta_1 - \beta_2} \frac{su^2 - sf^2}{sf^2 - sv^2} \frac{su}{sv}, \quad (48)$$

which determines the kink orbit flow. Note that this equation is identical to the equation in the HJ procedure that one must integrate to find (34). The subtle point, however, is that this flow is undefined,  $\frac{0}{0}$ , at the four foci:  $F_1, F_2, \bar{F}_1, \bar{F}_2$ , and all the NTK orbits pass through one of these dangerous points, see Figures 3(a) and 3(b). Like  $K_2$  topological kinks, the non-topological kink orbits solve (46)-(47) for a given sign combination before meeting at a focus and are solutions of (46)-(47) with another choice of signs after leaving these orbit intersections. Thus, non-topological kinks are classified as non-BPS in the terminology of previous Sections. We remark that in elliptic coordinates the pathology is not in the Hamilton characteristic function, as in spherical coordinates, but in the factors induced by the change to elliptic coordinates. The conclusion is that the energy of the NTK kinks must be computed piecewise along the orbit.

$$\begin{aligned} E_{K(\gamma_2)}^C &= 2\lambda \left| G^{(\beta_2)}(0) - G^{(\beta_2)}(v_B^\pm) \right| + \\ &\quad + 2\lambda \left| F^{(\beta_1)}(u_B^+) - F^{(\beta_1)}(u_B^-) \right| \\ &= 2\lambda R^2 |1 - \sigma| + 2\lambda R^2 |2\sigma| = 2\lambda R^2 (1 + \sigma) \end{aligned} \quad (49)$$

gives the kink energy as the action of the corresponding trajectory.

#### A. Singular $K_1$ and $K_2$ kinks: kink mass sum rule

A remake of the analysis of sub Section §III C about the BPS character of topological kinks in elliptic coordinates is illuminating. The  $K_1/K_1^*$  kink orbits lie in the  $v = 0$  line, splitting the two-halves of the elliptic rectangle:  $v_{K_1} = v_{K_1^*} = 0$ , see Figure 3(b). The first-order equations (46)-(47) on the  $K_1/K_1^*$  kink orbits ( $\beta_1 = 0$  gives kinks and  $\beta_1 = 1$  anti-kinks) and the  $K_1/K_1^*$  kink profiles in elliptic coordinates are:

$$\begin{aligned} \frac{du}{dx} &= -(-1)^{\beta_1} R \frac{su^2 - sf^2}{su} \\ u_{K_1}(x) &= u_{K_1^*}(x) = R \arccos[\sigma \tanh((-1)^{\beta_1} \sigma x)]. \end{aligned}$$

The  $K_1/K_1^*$  kink energy saturates the BPS bound:

$$E_{K_1}^C = \lambda \left| F^{(\beta_1)}(u_{K_1}(+\infty)) - F^{(\beta_1)}(u_{K_1}(-\infty)) \right| = 2\lambda R^2 \sigma.$$

The  $K_2/K_2^*$  kink orbits are the four edges of the elliptic rectangle:  $u_{K_2} = u_{K_2^*} = R\theta_f$ ,  $v_{K_2} = R\theta_f$ ,  $v_{K_2} = -R\theta_f$ ,  $u_{K_2} = u_{K_2^*} = R(\pi - \theta_f)$ , see again Figure 3(b). The  $K_2/K_2^*$  kinks are accordingly three-step trajectories in the elliptic rectangle.

I.  $-\infty < x < \log \tan \frac{\theta_f}{2}$  and  $u_{K_2}^I = u_{K_2^*}^I = R(\pi - \theta_f)$ , the first-order ODE, and the solutions are:

$$\beta_2 = 1, v' = R|sv|, v_{K_2}^I(x) = -v_{K_2^*}^I(x) = 2R \arctan e^x.$$

II.  $\log \tan \frac{\theta_f}{2} < x < \log \tan \frac{\pi - \theta_f}{2}$ ,  $v_{K_2}^{II} = -v_{K_2^*}^{II} = R\theta_f$ , the first-order ODE and the solution are:

$$\beta_1 = 0, u' = -Rsu, u_{K_2}^{II}(x) = u_{K_2^*}^{II}(x) = 2R \arctan e^{-x}.$$

III.  $\log \tan \frac{\pi - \theta_f}{2} < x < +\infty$ ,  $u_{K_2}^{III} = u_{K_2^*}^{III}$ , the first-order equation and the solutions are:

$$\beta_2 = 0, v' = -R|sv|, v_{K_2}^{III}(x) = -v_{K_2^*}^{III}(x) = 2R \arctan e^{-x}.$$

Anti-kinks are obtained by changing the choices of  $\beta_1$  and  $\beta_2$ . In any case, the  $K_2/K_2^*$  kink energy is not of the BPS form:

$$\begin{aligned} E_{K_2}^C &= \lambda \left| G^{(1)}(v(-\infty)) - G^{(1)}(v(\log \tan \frac{\theta_f}{2})) \right| \\ &\quad + \lambda \left| F^{(0)}(u(\log \tan \frac{\theta_f}{2})) - F^{(0)}(u(\log \cotan \frac{\theta_f}{2})) \right| \\ &\quad + \lambda \left| G^{(0)}(v(\log \cotan \frac{\theta_f}{2})) - G^{(0)}(v(+\infty)) \right| \\ &= \lambda R^2 |1 - \text{cf}| + \lambda R^2 |-2 \text{cf}| + \lambda R^2 |1 - \text{cf} + 1| = 2\lambda R^2. \end{aligned}$$

It is remarkable that these energies satisfy the following ‘‘Kink mass sum rule’’:

$$E_{K(\gamma_2)}^C = 2\lambda R^2 (1 + \sigma) = E_{K_2}^C + E_{K_1}^C \quad (50)$$

In fact, the  $|\gamma_2| \rightarrow \infty$  limit of the family of  $K_{\gamma_2}$  (NTK) kinks is compatible with equation (34) only at the edges of the elliptic rectangle (forming the  $K_2/K_2^*$  orbits) and the  $K_1/K_1^*$  orbit. Therefore, the  $K_1$  and  $K_2$  kinks form the boundary of the moduli space of NTK kinks in such a way that (50) shows this combination as one of the NTK kinks.

## X. SOLITARY SPIN WAVES

Field configurations that satisfy the Euler-Lagrange equations:

$$\begin{aligned} \frac{\partial A_a}{\partial t}(t, x) &= \sum_{b=1}^3 \left( \frac{\delta A_b}{\delta \phi_a}(t, x) - \frac{\delta A_a}{\delta \phi_b}(t, x) \right) \cdot \frac{\partial \phi_b}{\partial t}(t, x) \\ &= \sum_{b=1}^3 \sum_{c=1}^3 \varepsilon_{abc} B_c[\Phi(t, x)] \cdot \frac{\partial \phi_b}{\partial t}(t, x) \end{aligned}$$

are extremals of the ‘‘Wess-Zumino’’ action:

$$S_{\text{WZ}}[\Phi] = R^2 \int dt dx \sum_{a=1}^3 A_a[\Phi(t, x)] \frac{\partial \phi_a}{\partial t}(t, x).$$

In particular a “magnetic monopole” field  $B_a[\Phi(t, x)] = \frac{\phi_a(t, x)}{R^3}$  in the  $\mathbb{R}^3$  internal space where the  $\mathbb{S}^2$ -sphere is embedded is obtained by the choice of singular “vector potentials”:

$$\begin{aligned} A_1^\pm[\Phi(t, x)] &= -\frac{\phi_2}{\sqrt{\phi_1^2 + \phi_2^2 + \phi_3^2}(\phi_3 \pm \sqrt{\phi_1^2 + \phi_2^2 + \phi_3^2})} \\ A_2^\pm[\Phi(t, x)] &= \frac{\phi_1}{\sqrt{\phi_1^2 + \phi_2^2 + \phi_3^2}(\phi_3 \pm \sqrt{\phi_1^2 + \phi_2^2 + \phi_3^2})} \\ A_3^\pm[\Phi(t, x)] &= 0 \end{aligned}$$

$\vec{A}^+[\Phi(t, x)]$  is singular on the negative  $\phi_3$ -axis but a gauge transformation to  $\vec{A}^-[\Phi(t, x)]$  moves the Dirac string -henceforth a gauge artifact- to the positive  $\phi_3$ -axis. The scalar fields are constrained to live in the  $\phi_1^2(t, x) + \phi_2^2(t, x) + \phi_3^2(t, x) = R^2$  sphere, a surface where this magnetic flux is constant. Therefore, Stoke’s theorem tells us that  $S_{\text{WZ}} = R^2 \int dx \oint \sum_{a=1}^3 d\phi_a(x) A_a[\Phi(x)]$  is the area bounded by a closed curve in  $\mathbb{S}^2$ .

The important point is that the Euler-Lagrange equations for the sum of the two actions  $S_{\text{WZ}} + S$ , where  $S$  is the action of our model as defined in (4), are:

$$\frac{1}{R} \sum_{b=1}^3 \sum_{c=1}^3 \varepsilon_{abc} \phi_c \frac{\partial \phi_b}{\partial t} + \square \phi_a + \frac{\alpha_a^2}{\lambda^2} \phi_a = 0. \quad (51)$$

At the long wavelength limit, the ODE system (51) become the Landau-Lifshitz system of equations of ferromagnetism. The connection between the semi-classical (high-spin) limit of the Heisenberg model and the quantum non-linear  $\mathbb{S}^2$ -sigma model is well established [33].

### A. Spin waves

Plugging the constraint into (51), we find the system of two ODE’s:

$$\begin{aligned} & - \sum_{\alpha} \varepsilon_{\alpha\beta} \frac{\text{sg}\phi_3}{R} \left( \sqrt{R^2 - \sum_{\gamma} \phi_{\gamma} \phi_{\gamma}} \cdot \frac{\partial \phi_{\alpha}}{\partial t} \right. \\ & \quad \left. + \phi_{\alpha} \frac{\sum_{\gamma} \phi_{\gamma} \partial_t \phi_{\gamma}}{\sqrt{R^2 - \sum_{\gamma} \phi_{\gamma} \phi_{\gamma}}} \right) + \square \phi_{\beta} + m_{\beta}^2 \phi_{\beta} \\ & + \frac{\phi_{\beta}}{R^2 - \sum_{\gamma} \phi_{\gamma} \phi_{\gamma}} \left[ \frac{\sum_{\gamma} \phi_{\gamma} \partial^{\mu} \phi_{\gamma} + \sum_{\delta} \phi_{\delta} \partial_{\mu} \phi_{\delta}}{R^2 - \sum_{\gamma} \phi_{\gamma} \phi_{\gamma}} \right. \\ & \quad \left. - \sum_{\gamma} (\partial^{\mu} \phi_{\gamma} \partial_{\mu} \phi_{\gamma} + \phi_{\gamma} \square \phi_{\gamma}) \right] = 0. \quad (52) \end{aligned}$$

$\alpha, \beta, \gamma = 1, 2, m_1^2 = 1, m_2^2 = \sigma^2$ . The ground states are the homogeneous solutions of this system:  $\phi_1^0 = \phi_2^0 = 0, \phi_3^0 = \pm R$ , see Figure 7.

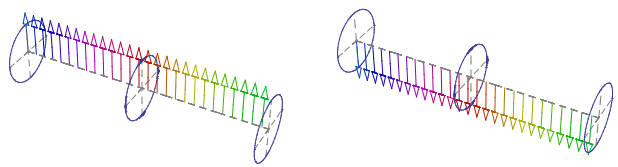


Figure 7: a) Ground state  $\phi_3^0 = R$ . All the spins are aligned pointing to the North Pole b) Ground state  $\phi_3^0 = -R$ . All the spins are aligned pointing to the South Pole.

The spin fluctuations  $\phi_1(t, x) = \delta\phi_1(t, x), \phi_2(t, x) = \delta\phi_2(t, x)$  around the ground state  $\phi_3(t, x) = R$  satisfy the linearized equations:

$$\begin{aligned} 0 &= \frac{\partial \delta\phi_2}{\partial t} + \frac{\partial^2 \delta\phi_1}{\partial t^2} - \frac{\partial^2 \delta\phi_1}{\partial x^2} + \delta\phi_1 \\ 0 &= -\frac{\partial \delta\phi_1}{\partial t} + \frac{\partial^2 \delta\phi_2}{\partial t^2} - \frac{\partial^2 \delta\phi_2}{\partial x^2} + \sigma^2 \delta\phi_2^2. \end{aligned}$$

Therefore, the spin waves:

$$\begin{aligned} \delta\phi_{\alpha}(t, x) &= \frac{1}{\sqrt{\lambda L}} \sum_k \frac{1}{\sqrt{\omega(k)}} (a_{\alpha}(k) e^{i\omega t - ikx} + \\ & \quad + a_{\alpha}^*(k) e^{-i\omega t + ikx}) \end{aligned} \quad (53)$$

satisfying periodic boundary conditions  $\delta\phi_{\alpha}(t, x) = \delta\phi_{\alpha}(t, x + \lambda L)$  are solutions of (53) for the frequencies complying with the homogeneous system of algebraic equations:

$$\begin{pmatrix} -\omega^2 + k^2 + 1 & i\omega \\ -i\omega & -\omega^2 + k^2 + \sigma^2 \end{pmatrix} \begin{pmatrix} a_1(k) \\ a_2(k) \end{pmatrix} = \begin{pmatrix} 0 \\ 0 \end{pmatrix}. \quad (54)$$

At the long wavelength limit  $\omega^2 \ll \omega$ , (54) is tantamount to the non-relativistic dispersion law

$$\omega^2(k^2) = (k^2 + 1)(k^2 + \sigma^2)$$

characteristic of ferromagnetic materials, although the quadratic potential energy density prevents the standard  $\omega(k) = k^2$  form.

### B. Bloch and Ising walls

One may check that the  $K_1/K_1^*$  kinks (11) solve the static Landau-Lifshitz equations (52) on the  $\phi_1 = 0$  orbit:

$$\frac{d^2 \phi_2}{dx^2} = \frac{-\phi_2}{R^2 - \phi_2^2} \left[ \frac{(\phi_2 \frac{d\phi_2}{dx})^2}{R^2 - \phi_2^2} + \left( \frac{d\phi_2}{dx} \right)^2 + \phi_2 \frac{d^2 \phi_2}{dx^2} \right] + \sigma^2 \phi_2$$

The  $K_1/K_1^*$  kinks of the non-linear sigma model are consequently solitary spin waves of this non-relativistic system, see Figure 8.

Simili modo, the  $K_2/K_2^*$  kinks (12) solve (52) along the  $\phi_2 = 0$  kink orbit:

$$\frac{d^2 \phi_1}{dx^2} = \frac{-\phi_1}{R^2 - \phi_1^2} \left[ \frac{(\phi_1 \frac{d\phi_1}{dx})^2}{R^2 - \phi_1^2} + \left( \frac{d\phi_1}{dx} \right)^2 + \phi_1 \frac{d^2 \phi_1}{dx^2} \right] + \phi_1$$

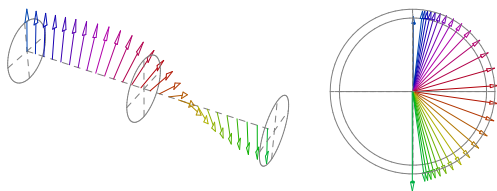


Figure 8: Graphic arrow representation of the  $K_1$  kinks: a)  $K_1$  spin chain. b) Perspective from one component of the boundary of  $\mathbb{S}^2 \times \mathbb{R}$  showing how the spin flip happens by means of a  $\pi$ -rotation around the  $\phi_1$ -axis.

and are also spin solitary waves in this system, see Figure 9.

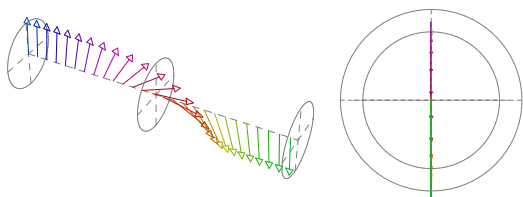


Figure 9: Graphic arrow representation of the  $K_2$  kink a)  $K_2$  spin chain. b) Perspective from one component of the boundary of  $\mathbb{S}^2 \times \mathbb{R}$  showing a forward spin flip.

Finally, because the system of ODE's giving static solutions of the (51) PDE system is the same as the static field equations of the non-linear  $\mathbb{S}^2$ -sigma model, the NTK kinks are also solitary spin waves, see Figure 10.

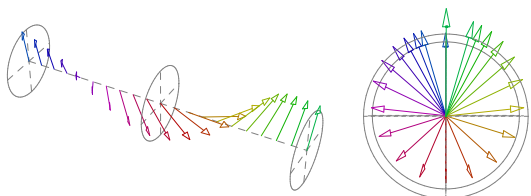


Figure 10: Graphic arrow representation of  $K_{\gamma_2}$  kinks: a)  $K_{\gamma_2}$  spin chain. b) Perspective from the boundary of  $\mathbb{S}^2 \times \mathbb{R}$  showing the  $2\pi$  rotation around the  $\phi_1$ -axis of the spin to come back to the initial ground state.

In sum, understood as solitary spin waves  $K_1/K_1^*$  kinks are Bloch walls whereas  $K_2/K_2^*$  kinks are Ising walls describing interfaces between ferromagnetic domains, see [34], [35]. In this model we have thus found a moduli space of solitary waves with an structure almost identical to the structure of the space of solitary waves of the XY model described in Reference [34]. There are Bloch and Ising walls and a one-parametric family of NTK kinks that are non-linear superpositions of one Bloch and one Ising wall with arbitrary separation between their centers. From the stability analysis performed in previous

Sections, it is clear that only the Bloch walls are stable and saturate the Bogomolny bound. Things are different at the  $\sigma = 1$  limit where all the kinks are topological, Bloch walls, and saturate the Bogomolny bound. In this latter case the structure of the kink space is akin to the kink space structure of the BNRT model [36], see [37], [38], [14]. There is a one-parametric family of degenerate Bloch walls saturating the Bogomolny bound.

## XI. FURTHER COMMENTS: SUPERSYMMETRY AND STABILITY

Finally, we briefly explore the possibility of embedding our bosonic model with its moduli space of kinks in a broader supersymmetric framework. It turns out that the simpler  $\mathcal{N} = 1$ ,  $d = 1 + 1$  SUSY version of the massive non-linear  $\mathbb{S}^2$ -sigma model only exists if the masses of the pseudo Nambu-Goldstone bosons are equal ( $\sigma = 1$ ). It also seems difficult to build more exotic possibilities coming from dimensional reduction of models of Kahler or hyper-Kahler nature because the potential energy density is not compatible with complex structures when  $\sigma \neq 1$ .

### A. Isothermal coordinates

It is convenient to introduce isothermal coordinates in the chart  $\mathbb{S}^2 - \{(0, 0, -R)\}$ , which are obtained via stereographic projection from the South Pole:

$$\begin{aligned} \chi^1 &= \frac{\phi_1}{1 + \frac{\phi_3}{R}} = \frac{R\phi_1}{R + \text{sg}(\phi_3)\sqrt{R^2 - \phi_1^2 - \phi_2^2}} \\ \chi^2 &= \frac{\phi_2}{1 + \frac{\phi_3}{R}} = \frac{R\phi_2}{R + \text{sg}(\phi_3)\sqrt{R^2 - \phi_1^2 - \phi_2^2}}. \end{aligned} \quad (55)$$

Conversely,

$$\begin{aligned} \phi_1 &= \frac{2R^2\chi^1}{R^2 + \chi^1\chi^1 + \chi^2\chi^2} \\ \phi_2 &= \frac{2R^2\chi^2}{R^2 + \chi^1\chi^1 + \chi^2\chi^2} \\ \phi_3 &= R \frac{R^2 - \chi^1\chi^1 - \chi^2\chi^2}{R^2 + \chi^1\chi^1 + \chi^2\chi^2}. \end{aligned}$$

The geometric data of the sphere in this coordinate system are:

$$\begin{aligned} ds^2 &= \frac{4R^4}{(R^2 + \chi^1\chi^1 + \chi^2\chi^2)^2} (d\chi^1 d\chi^1 + d\chi^2 d\chi^2) \\ \Gamma_{11}^1 &= -\Gamma_{22}^1 = \Gamma_{12}^2 = \Gamma_{21}^2 = \frac{-2\chi^1}{R^2 + \chi^1\chi^1 + \chi^2\chi^2}, \\ \Gamma_{22}^2 &= -\Gamma_{11}^2 = \Gamma_{12}^1 = \Gamma_{21}^1 = \frac{-2\chi^2}{R^2 + \chi^1\chi^1 + \chi^2\chi^2}, \\ R_{1122}^1 &= R_{2111}^2 = \frac{-4R^4}{(R^2 + \chi^1\chi^1 + \chi^2\chi^2)^2} \\ R_{2112}^1 &= R_{1211}^2 = \frac{4R^4}{(R^2 + \chi^1\chi^1 + \chi^2\chi^2)^2}. \end{aligned}$$

The action is:

$$S[\chi^1, \chi^2] = \int dx^2 \frac{2R^4}{(R^2 + \chi^1\chi^1 + \chi^2\chi^2)^2} \cdot [\partial_\mu \chi^1 \partial^\mu \chi^1 + \partial_\mu \chi^2 \partial^\mu \chi^2 - (\chi^1\chi^1 + \chi^2\chi^2)],$$

whereas the  $K_1$  kinks are given by:

$$\chi_{K_1}^1(x) = 0, \quad \chi_{K_1}^2(x) = \pm R \exp[\pm\sigma(x - x_0)], \quad (56)$$

and we rewrite the second order fluctuation operator around the  $K_1$  kink ( $\chi_{K_1}^1(x) = 0, \chi_{K_1}^2(x) = Re^{-\sigma x}$ ) in the form:

$$\begin{aligned} \Delta_{K_1} \eta &= - \left( \frac{d^2 \eta^1}{dx^2} + 2\sigma(1 - \tanh \sigma x) \frac{d\eta^1}{dx} \right. \\ &\quad \left. - (1 - 2\sigma^2 + 2\sigma^2 \tanh \sigma x) \eta^1 \right) \frac{\partial}{\partial \chi^1} - \left( \frac{d^2 \eta^2}{dx^2} + \right. \\ &\quad \left. + 2\sigma(1 - \tanh \sigma x) \frac{d\eta^2}{dx} + \sigma^2(1 - 2 \tanh \sigma x) \eta^2 \right) \frac{\partial}{\partial \chi^2}. \end{aligned}$$

In a parallel frame  $\mu = \mu^1(x) \frac{\partial}{\partial \chi^1} + \mu^2(x) \frac{\partial}{\partial \chi^2} \in \Gamma(T\mathbb{S}^2|_{K_1})$ ,  $\frac{d\mu^i}{dx} + \Gamma_{jk}^i(\chi K) \chi_K^j \mu^k = 0$ , along the  $K_1$  kink orbit:

$$\begin{aligned} \frac{d\mu^1}{dx} + \sigma(1 - \tanh) \mu^1(x) = 0 &\Rightarrow \mu^1(x) = 1 + e^{-2\sigma x} \\ \frac{d\mu^2}{dx} + \sigma(1 - \tanh) \mu^2(x) = 0 &\Rightarrow \mu^2(x) = 1 + e^{-2\sigma x}. \end{aligned}$$

we recover the Pösch-Teller operators:

$$\begin{aligned} \Delta_{K_1} \eta &= \left( -\frac{d^2 \eta^1}{dx^2} + (1 - \frac{2\sigma^2}{\cosh^2 \sigma x}) \eta^1 \right) (1 + e^{-2\sigma x}) \frac{\partial}{\partial \chi^1} \\ &\quad + \left( -\frac{d^2 \eta^2}{dx^2} + (\sigma^2 - \frac{2\sigma^2}{\cosh^2 \sigma x}) \eta^2 \right) (1 + e^{-2\sigma x}) \frac{\partial}{\partial \chi^2} \quad (57) \end{aligned}$$

Note that now the  $K_1$  orbits are the positive and negative ordinate half-axes, the stereographic projections of the  $\varphi = \frac{\pi}{2}$  and  $\varphi = \frac{3\pi}{2}$  half-meridians, such that fluctuations orthogonal to the orbit run in the direction of the abscissa axis.

## B. The $\mathcal{N} = 1$ massive SUSY sigma model

In Reference [40] we analyzed the relationship of the complete solution of the Hamilton-Jacobi equation for zero energy and the superpotential of a supersymmetric associated classical mechanical system. Thus, we are tempted to use the Hamilton characteristic function

$$W^{(\beta_1, \beta_2)}(\chi) = \frac{(-1)^{\beta_1} R^2}{R^2 + \chi^1\chi^1 + \chi^2\chi^2} \cdot \sqrt{(\sigma_+(\beta_2)R^2 + \sigma_-(\beta_2)(\chi^1\chi^1 + \chi^2\chi^2))^2 - 4\bar{\sigma}^2 R^2 \chi^1\chi^1}, \quad (58)$$

$\sigma_\pm(\beta_2) = 1 \pm (-1)^{\beta_2} \sigma$ , to build the  $\mathcal{N} = 1$  SUSY extension of our massive non-linear  $\mathbb{S}^2$ -sigma model. On one hand we have that:

$$\frac{1}{2} g^{ij} \frac{\partial W^{(\beta_1, \beta_2)}}{\partial \chi^i} \cdot \frac{\partial W^{(\beta_1, \beta_2)}}{\partial \chi^j} = \frac{2R^2(\chi^1\chi^1 + \sigma^2\chi^2\chi^2)}{(R^2 + \chi^1\chi^1 + \chi^2\chi^2)^2},$$

$\forall \beta_1, \beta_2$ . On the other hand (58) is free of branch points only for  $\sigma = 1$ . Supersymmetry does not allow superpotentials with branch points and it seems that Hamilton-Jacobi characteristic functions are compatible with a weaker form called pseudo-supersymmetry in [41]. We close our eyes to this fact for a moment and proceed to formally build the  $\mathcal{N} = 1$  SUSY extension of our model using (58).

There are also two Majorana spinor fields:

$$\psi^i(x^\mu) = \begin{pmatrix} \psi_1^i(x^\mu) \\ \psi_2^i(x^\mu) \end{pmatrix}, \quad (\psi_\alpha^i)^* = \psi_\alpha^i, \quad \alpha = 1, 2.$$

We choose the Majorana representation  $\gamma^0 = \sigma^2, \gamma^1 = i\sigma^1, \gamma^5 = \sigma^3$  of the Clifford algebra  $\{\gamma^\mu, \gamma^\nu\} = 2g^{\mu\nu}$  and define the Majorana adjoints as:  $\bar{\psi}^i = (\psi^i)^t \gamma^0$ . The action of the supersymmetric model is:

$$S = \int \frac{dx^2}{2} \left\{ g_{ij} \left( \partial_\mu \chi^i \partial^\mu \chi^j + i\bar{\psi}^i \gamma^\mu (\partial_\mu \psi^j + \Gamma_{lk}^j \partial_\mu \chi^k \psi^l) \right) - \frac{1}{6} R_{ijkl} \bar{\psi}^i \psi^j \bar{\psi}^l \psi^k - g^{ij} \frac{\partial W}{\partial \chi^i} \frac{\partial W}{\partial \chi^j} - \bar{\psi}^i \frac{D\partial W}{\partial \chi^i \partial \chi^j} \psi^j \right\},$$

where  $\frac{D\partial W}{\partial \chi^i \partial \chi^j} = \frac{\partial^2}{\partial \chi^i \partial \chi^j} + \Gamma_{ij}^k \frac{\partial W}{\partial \chi^k}$ . The spinor supercharge

$$Q = \int dx g_{ij} \left( \gamma^\mu \gamma^0 \psi^i \partial_\mu \chi^j + i\gamma^0 \psi^i g^{jk} \frac{\partial W}{\partial \chi^k} \right) \quad (59)$$

acts on the configuration space and leaves the action invariant. Time-independent finite energy configurations complying with

$$\frac{d\chi^i}{dx} = g^{ij} \frac{\partial W}{\partial \chi^j}, \quad \psi_1^i(x) = -\psi_2^i(x) \quad (60)$$

annihilates the supercharge combination  $Q_1 + Q_2$  and these solutions might be interpreted as  $\frac{1}{2}$  BPS states in



this supersymmetric framework. In particular, the SUSY  $K_1$  kinks

$$\begin{aligned} \chi_{K_1}^1(x) &= 0 \quad , \quad \chi_{K_1}^2 = \pm R e^{\pm \sigma x} \\ \psi_{K_1}^1(x) &= \begin{pmatrix} 0 \\ 0 \end{pmatrix} \quad , \quad \psi_{K_1}^2(x) = \pm \sigma R e^{\pm \sigma x} \begin{pmatrix} 1 \\ -1 \end{pmatrix} \end{aligned}$$

satisfy (60) (with appropriate choices of  $\beta_1, \beta_2$ ). Note that  $\psi_{K_1}^2(x)$  is the SUSY partner of  $\chi_{K_1}^2(x)$  under the action of the broken SUSY supercharge  $Q_1 - Q_2$ . We also remark that

$$\frac{d\chi_{K_1}^2}{dx} = \pm \sigma R e^{\pm \sigma x} = \pm \sigma R (1 + e^{\pm 2\sigma x}) \cdot \frac{1}{\cosh \sigma x} \quad ,$$

i.e., the fermionic partner in the SUSY kink is the zero mode of the second order fluctuation operator back from the parallel frame to the  $K_1$  orbit.

### C. Fermionic fluctuations

The Dirac equation ruling the small fermionic fluctuations on the  $K_1$  kink reads:

$$\begin{aligned} D\delta\psi^i(t, x) &= i(\gamma^0\partial_0 - \gamma^1\partial_1)\delta\psi^i(t, x) \\ &\quad - i\gamma^1\Gamma_{jk}^i(\chi_{K_1})\partial_1\chi_{K_1}^j(x)\delta\psi^k(t, x) \\ &\quad + g^{ij}(\chi_{K_1})\frac{D\partial W}{\partial\chi^j\partial\chi^k}(\chi_{K_1})\delta\psi^k(t, x) \end{aligned} \quad (61)$$

Acting on (61) with the adjoint Dirac operator, the search for solutions of  $D^\dagger D\delta\psi^i(t, x) = 0$  of the stationary form  $\delta\psi^i(t, x) = e^{i\omega t}\delta\varrho^i(x, \omega)$  requires us to deal with the following ODE system:

$$\begin{aligned} -\frac{d^2}{dx^2}\delta\varrho^i(x) + g^{ij}\frac{D\partial W}{\partial\chi^j\partial\chi^k} \cdot g^{kl}\frac{D\partial W}{\partial\chi^l\partial\chi^m}\delta\varrho^m(x) \\ + R_{jkl}^i\frac{d}{dx}\chi_{K_1}^j\frac{d}{dx}\chi_{K_1}^k\delta\varrho^l(x) \\ - i\gamma^1 g^{ij}\frac{\partial W}{\partial\chi^j} \cdot g^{kl}\frac{D^2\partial W}{\partial\chi^k\partial\chi^l\partial\chi^m}\delta\varrho^m(x) = \omega^2\delta\varrho^i(x) \end{aligned}$$

valued at  $\chi = \chi_{K_1}$ .

On eigenspinors of  $-i\gamma^1 = \sigma^1$ ,  $\delta\varrho_1^i(x) = \pm\delta\varrho_2^i(x) = \delta\varrho_\pm^i(x)$ , the above spectral ODE system reduce to the (symbolically written) pair of equations:

$$\Delta_{K_1}^\pm \delta\varrho_\pm = \left[ -\frac{d^2}{dx^2} + W'' \otimes W'' + R \pm W' \otimes W''' \right] \delta\varrho_\pm \quad (62)$$

$\Delta_{K_1}^+$  is exactly equal to the second order differential operator ruling the bosonic fluctuations. Therefore, in the parallel frame to the  $K_1$  orbit we write  $\Delta_{K_1}^+$  in matrix form:

$$\Delta_{K_1}^+ = \begin{pmatrix} -\frac{d^2}{dx^2} + 1 - \frac{2\sigma^2}{\cosh^2\sigma x} & 0 \\ 0 & -\frac{d^2}{dx^2} + \sigma^2 - \frac{2\sigma^2}{\cosh^2\sigma x} \end{pmatrix}.$$

In the same frame  $\Delta_{K_1}^-$  is the intertwined partner, see [19]:

$$\Delta_{K_1}^- = \begin{pmatrix} -\frac{d^2}{dx^2} + 1 & 0 \\ 0 & -\frac{d^2}{dx^2} + \sigma^2 \end{pmatrix}.$$

If  $\sigma \neq 1$ , there is a bound state in  $\Delta_{K_1}^+$  of energy  $1 - \sigma^2$  unpaired with an eigenstate of the same energy in  $\Delta_{K_1}^-$ , a fact incompatible with supersymmetry as we expected from the use of the complete solution of the Hamilton-Jacobi equation as superpotential, closing our eyes to the fact that, related to the instability of  $NTK$  and  $K_2$  kinks, the Hamilton characteristic function has branching points at the foci defining the elliptic coordinate system. A similar problem arose in [42] and [43] where meromorphic Hamilton characteristic functions have been found. It is an open problem to explore whether or not these milder singularities allow the use of these Hamilton characteristic functions as superpotentials to extend the bosonic models dealt with in [42], [43] to the supersymmetric framework.

If the masses are equal ( $\sigma = 1$ ), however, the Hamilton characteristic function is free of branching points and the unpaired states are zero modes. The  $\mathcal{N} = 1$  SUSY model is correct and we can apply the SUSY version of the Cahill-Comtet-Glauber formula proposed in [44] to find the same one-loop correction to the SUSY  $\mathbb{S}^2$  kink as given in [19]:

$$\Delta E_{K_1}^{\text{SUSY}}(\sigma = 1) = -\frac{\lambda}{2\pi} \sum_{i=1}^2 (\sin \nu_i^+ - \nu_i^+ \cos \nu_i^+) = -\frac{\lambda}{\pi}.$$

Here  $\nu_1^+ = \nu_2^+ = \arccos(0) = \frac{\pi}{2}$  are the angles obtained from the bound states of  $\Delta_{K_1}^+$ . There are no bound states in the spectrum of  $\Delta_{K_1}^-$ .

## XII. ACKNOWLEDGEMENTS

We are grateful to M. Santander, S. Woodford, I. Barashenkov, M. Nitta, P. Letelier, D. Bazeia, and Y. Fedorov for informative and illuminating electronic/ordinary mail correspondence and/or oral conversations on several issues concerning this work. Any misunderstanding is the authors's own responsibility.

We also thank the Spanish Ministerio de Educacion y Ciencia and Junta de Castilla y Leon for partial support under grants FIS2006-09417 and GR224.

- 
- [1] A. Alonso Izquierdo, M. A. Gonzalez Leon, and J. Mateos Guilarte, Phys. Rev. Lett. **101** (2008) 131602
- [2] K. Cahill, A. Comtet, and R. Glauber, Phys. Lett. **64B**(1976) 283-285
- [3] E. R. C. Abraham and P. K. Townsend, Phys. Lett. **B291** (1992) 85-88
- [4] E. R. C. Abraham and P. K. Townsend, Phys. Lett. **B295** (1992) 225-232
- [5] M. Arai, M. Naganuma, M. Nitta, and N. Sakai, Nucl. Phys. **B652** (2002) 35-71
- [6] N. Dorey, JHEP 9811 (1998) 005
- [7] R. A. Leese, Nucl. Phys. **B366** (1991) 283-314
- [8] E. Abraham, Phys. Lett. **B278** (1992) 291-296
- [9] J. P. Gauntlet, R. Portugues, D. Tong, P. K. Townsend, Phys. Rev. **D63** (2001) 085002
- [10] Y. Isozumi, M. Nitta, K. Oshasi, N. Sakai, Phys. Rev. **D71** (2005) 065018
- [11] M. Eto, Y. Isozumi, M. Nitta, K. Oshasi, N. Sakai, Jour. Phys. **A39** (2006) R315-R392
- [12] M. Eto, and N. Sakai, Phys. Rev. **D68** (2003) 125001
- [13] D. Bazeia, and A. R. Gomes, JHEP **05**(2004) 012
- [14] A. de Souza Dutra, A. C. Amaro de Faria, and M. Holt, Phys. Rev. **D78**(2008) 043526
- [15] S. F. Coleman, Comm. Math. Phys. **31** (1973) 259
- [16] S. F. Coleman, "Aspects of symmetry", Cambridge University Press, 1985, Chapter 6: "Classical lumps and their quantum descendants"
- [17] R. Rajaraman, Phys. Rev. Lett. **42** (1979) 200
- [18] L. J. Boya, and J. Casahorran, Ann. Phys. **196** (1989) 361-385
- [19] C. Mayrhofer, A. Rehban, P. van Nieuwenhuizen, and R. Wimmer, JHEP (2007) 0709:069
- [20] A. Alonso Izquierdo, W. Garcia Fuertes, M. A. Gonzalez Leon, and J. Mateos Guilarte, Nucl. Phys **B 638** (2002) 378-404
- [21] A. Alonso Izquierdo, W. Garcia Fuertes, M. A. Gonzalez Leon, and J. Mateos Guilarte, Nucl. Phys **B 635** (2002) 525-557
- [22] A. Alonso Izquierdo, W. Garcia Fuertes, M. A. Gonzalez Leon, and J. Mateos Guilarte, Nucl. Phys **B 681** (2004) 163-194
- [23] A. Alonso Izquierdo, and J. Mateos Guilarte, Physica **D 237** (2008)3263-3291
- [24] S. F. Coleman, S. Park, A. Neveu, and C. Sommerfield, Phys. Rev. **D15** (1977) 544
- [25] P. Morse and H. Feshbach, "Methods of Theoretical Physics", Volume I, McGraw Hill, New York, 1953
- [26] B. Dubrovine, Russ. Math. Surv. **36:2**(1981)11-80
- [27] E. Bogomolny, Sov. J. Nucl. Phys.**24** (1976) 449
- [28] A. Perelomov, *Integrable Systems of Classical Mechanics and Lie Algebras*, Birkhauser, (1992)
- [29] H. Ito, Phys. Lett. **112A** (1985) 119
- [30] A. Alonso Izquierdo, M. A. Gonzalez Leon, J. Mateos Guilarte, J. Phys. **A31** (1998) 209
- [31] H. Ito, H. Tasaki, Phys. Lett. **A113** (1985) 179
- [32] J. Mateos Guilarte, Ann. Phys. **188** (1988) 307
- [33] F. D. M. Haldane, Phys. Rev. Lett. **50** (1983) 1153
- [34] S. R. Woodford, and I. V. Barashenkov, J. Phys. A: Math. Teor. **41** (2008) 185203
- [35] I. V. Barashenkov, S. R. Woodford, and E. V. Zemlyanaya, Phys. Rev. Lett. **90** (2003) 054103
- [36] D. Bazeia, J. R. Nascimento, R. Ribeiro, and D. Toledo, J. Phys. A: Math. Gen. **30**(1997) 8157
- [37] M. A. Shifman, and M. B. Voloshin, Phys. Rev. **D57** (1998) 2590
- [38] A. Alonso Izquierdo, M. A. Gonzalez Leon, J. Mateos Guilarte, Phys. Rev. **D65** (2002) 085012
- [39] A. Alonso Izquierdo, M. A. Gonzalez Leon, J. Mateos Guilarte, Nonlinearity **15** (2002) 1097
- [40] A. Alonso Izquierdo, M. A. Gonzalez Leon, J. Mateos Guilarte, and M. de la Torre Mayado, Ann. Phys. **308** (2003) 664-691
- [41] P. K. Townsend, Class. Quant. Grav. **25** (2008)045017
- [42] V. Afonso, D. Bazeia, M. A. Gonzalez Leon, L. Losano, and J. Mateos Guilarte, Phys. Lett. **B662**(2008)74-79
- [43] V. Afonso, D. Bazeia, M. A. Gonzalez Leon, L. Losano, and J. Mateos Guilarte, Nucl. Phys. **B810**[FS] (2009)427-459
- [44] L. J. Boya, and J. Casahorran, Jour. Phys. **A23** (1990) 1645